Westward Ho! Evidence of Longitudinal Migration in Silver-haired Bats from Hydrogen, Carbon, and Nitrogen Stable Isotopes.

by

Kyle R. Nelson
B.Sc., University of Victoria, 2017

A Thesis Submitted in Partial Fulfillment of the
Requirements for the Degree of

MASTER OF SCIENCE

in the School of Environmental Studies

© Kyle Nelson, 2023
University of Victoria

All rights reserved. This thesis may not be reproduced in whole or in part, by photocopying or other means, without the permission of the author.

Westward Ho! Evidence of Longitudinal Migration in Silver-haired Bats from Hydrogen, Carbon, and Nitrogen Stable Isotopes.

by

Kyle R. Nelson

B.Sc., University of Victoria, 2017

Supervisory Committee

Dr. Brian Starzomski, Supervisor

(School of Environmental Studies)

Dr. Jason Fisher, Departmental Member

(School of Environmental Studies)

ABSTRACT

Migration is an energetically demanding process and North America's migratory bats are facing the additional pressure of mortality from rapidly expanding wind energy facilities. Knowledge of bat migrations can be used to identify critical habitat and direct siting and mitigation measures to reduce the impact of wind turbines, but methods to study these movements remain limited. Silver-haired bats (*Lasionycteris noctivagans*) are a widely distributed bat species in North America that undergoes substantial migrations between their summer and winter locations. Studying these movements has long been a challenge, but technological advances such as the application of stable isotopes to animal migration studies make this more feasible. To date, the majority of the research conducted on silver-haired bat migrations has been focused on their movements east of the Continental Divide. Coastal influences and complex topography have been an impediment to the utilization of stable isotopes in bat migration studies west of this divide. To overcome this challenge, I systematically sampled silver-haired bats for multiple stable isotopes, hydrogen (δ^2H), carbon (δ^{13}C), and nitrogen (δ^{15}), across a broad range of geography representative of western North America. Using Generalized Additive Models, I found geographical and climatological correlates of δ^2H, δ^{13}C, and δ^{15}N distributions and used these to create the first species-specific stable isotope distribution maps (isoscapes) for silver-haired bats in western North America. I applied these isoscapes in a continuous-surface assignment framework to determine the most-probable migratory origins of silver-haired bats overwintering in coastal regions of southern British Columbia and western Washington State. The stable isotope signatures of these individuals indicated that the majority of them had spent their summers across a broad area further to the east, providing the first empirical evidence of longitudinal migration in silver-haired bats and indicating that

coastal areas of British Columbia and Washington State are important overwintering habitat for this species. This work proves that with careful selection of both the samples and stable isotopes used, along with thoughtful consideration of the underlying geographic and climatological processes that drive their ratio distributions, stable isotopes can be used to track seasonal movements of animals in regions of complex topography. These results also emphasize the importance of coastal areas to overwintering silver-haired bats, and the need for strict regulation of wind turbines sited along likely migratory corridors connecting these coastal areas to interior summer habitat.

Contents

List of Tables

List of Figures

ACKNOWLEDGEMENTS

I am grateful for the funding bodies that enabled me to undertake this endeavour: the Natural Sciences and Engineering Research Council of Canada, the University of Victoria, the School of Environmental Studies, and the Western Bat Working Group. I would also like to thank the many institutions and curators that kindly permitted me to give their precious specimens a hair cut in the name of science.

A huge thank you to my supervisor, Dr. Brian Starzomski, for his guidance and incredible patience through this process. I am especially appreciative of his support for my burgeoning career, which thanks to this process has grown into something very fulfilling and batty. My thanks also goes to Dr. Jason Fisher for his swift responses whenever I would re-emerge from the darkness inevitably wanting something from him.

Thank you to my fellow Starzombies, my incredible Pear cohort, and the ES community as a whole. Special thank you to Kalina for getting through the early days with me, and to Jordan for always being up for a beer and sharing wisdom beyond his years.

It was a blessing and a curse to do most of this while actively employed, but that is the cost of having a workplace that was too good to give up. A thank you to my colleagues at Parks Canada, particularly the long list of supervisors that were wonderfully understanding and supportive.

I am incredibly thankful to my family. They may not be exactly sure what this all was about, but they instilled in me the work ethic and inquisitiveness that was essential to getting me through this when so many distractions could have prevailed.

Finally, thank you to Clare for going above and beyond to help me see this through, whether it was troubleshooting code, listening to me gripe, delivering much-needed refreshments, or most importantly of all, making me smile.

DEDICATION

To Dot,

You brought me laughter and joy during the lowest points in this process. I miss you every day.

Chapter 1

General Introduction

With over 1400 species spread across every continent except Antarctica, bats have proven to be incredibly adaptable to a variety of environmental conditions. From pollinating plants and dispersing seeds in tropical climates, to controlling insect populations in the temperate regions of the globe, bats provide essential services to the habitats that they occupy (Kunz et al., 2011). The majority of North America's bats are insectivores, and some of these species have adopted migrations of hundreds or thousands of kilometers to survive the annual decline in insect prey that comes with winter in northern regions of the continent. Humans have altered landscapes in ways that present new threats to bats as they undergo these migrations (Arnett et al., 2016). A better understanding of the spatial patterns of bat migration will help identify areas of potential conflict between migratory bats and their threats, contributing to more effective conservation of bat populations (Kunz et al., 2007). Studying these movements has long been a challenge, but technological advances such as the application of stable isotopes to animal migration studies make this more feasible (Cryan et al., 2014; Campbell et al., 2020). The silver-haired bat (*Lasionycteris noctivagans*) is an insectivorous, tree-roosting species that undergoes

substantial migrations between summer and winter habitats. Although silver-haired bats are ubiquitous across much of North America, the majority of the research conducted on their migrations has been focused on movements east of the Continental Divide (Baerwald et al., 2014; Fraser et al., 2017). Rapid development in the western extent of the silver-haired bat's range poses a threat to the species and there is a pressing need to determine their migratory movements in the face of these threats. With this thesis, I set out to use stable isotopes of common environmental elements to develop a novel tool for revealing silver-haired bat migrations in western North America.

1.1 Threats to Bats

Bats are rapidly overcoming the misleading historical stigma of frightening creatures of the night to be recognized for the fascinating mammals that they are. However, globally their populations face a number of threats and many species are in decline. Over one third of all bat species are identified as threatened or data deficient by the International Union for Conservation of Nature (Frick et al., 2020). Some of the most widespread threats to bat populations imperil their food and habitat needs. Deforestation and harmful silviculture practices diminish the quality of both foraging and roosting habitat (Law et al., 2016). The disturbance and destruction of subterranean features such as caves and mines also degrades roosting opportunities and threatens critical winter hibernation sites (Furey and Racey, 2016). Insect populations are diminishing globally (Cardoso et al., 2020; Wagner et al., 2021), and this has implications for insectivorous bat species that depend on them for food. Sustaining flight is energetically costly, and declining insect densities mean that bats must expend more energy to meet their needs (Gonsalves

et al., 2013). These needs are not to be underestimated. During pregnancy and lactation, insectivorous bats can consume 70-100% of their own body weight in prey in a single night (Kurta et al., 1989; Kunz et al., 1995). Losses of habitat and food resources threaten to undermine foundational elements of the environment essential for sustained bat populations.

For bats in North America, degradation of habitat exacerbates the serious and expanding threat posed by white-nose syndrome (WNS). WNS, and its causative fungus *Pseudogymnoascus destructans* (*Pd*), are native to Europe but were found to be infecting bats in New York State in 2006 (Blehert et al., 2009). WNS has since spread across much of North America, having a devastating effect on bat populations. *Pd* infects a bat's skin, causing irritations that wear down an individual's energy reserves over the course of winter hibernation, often leading to death (Frick et al., 2010). The smaller *Myotis* and *Perimyotis* species, which depend on hibernation as their overwintering strategy, are especially impacted. The population declines caused by WNS have led to the listing of the northern long-eared bat (*Myotis septentrionalis*) as Endangered in the United States and Canada (Environment Canada, 2015; USFWS, 2022), and the tricoloured bat (*Perimyotis subflavus*) and little brown bat (*Myotis lucifugus*) as Endangered in Canada (Environment Canada, 2015). A concerted effort is being made by researchers to get ahead of the spread of WNS in North America by determining its pathways of spread across the continent and possible intervention measures to treat the disease (Foley et al., 2011; Rocke et al., 2019; Vonhof et al., 2019; Fletcher et al., 2020).

While WNS is less of a threat to North America's larger migratory bats, namely the silver-haired bat, hoary bat (*Lasiurus cinereus*), and eastern red bat (*Lasiurus borealis*), these species suffer significant mortality due to the wind energy industry (Arnett and Baerwald, 2013). It was estimated that between 600,000 (Hayes, 2013)

and 888,000 (Smallwood, 2013) bats were killed by wind turbines in the United States in 2012 alone, with that number likely increasing with the expansion of the industry. A number of theories have been posited as to why migratory bats bear the brunt of turbine-related fatalities. The habitat modification necessary for turbine construction may be creating attractive travel and foraging conditions (Kunz et al., 2007). It could be that migratory bats favour linear features for migration (Furmankiewicz and Kucharska, 2009; Wieringa et al., 2021), and this coincides with preferred turbine sites, or it could be that bats are attracted to turbines on the landscape, possibly mistaking them for tall trees that serve as roosts or social gathering points (Jameson and Willis, 2014). Regardless of the cause, the threat is real and well-supported by evidence (Arnett et al., 2008; Arnett and Baerwald, 2013; Hayes, 2013; Zimmerling and Francis, 2016). It is predicted that at current rates of decline, the hoary bat population could be reduced by 90% in the next 44 years (Frick et al., 2017). It is largely due to the threat posed by wind turbines that the Committee on the Status of Endangered Wildlife in Canada recommended listing the country's populations of migratory bat species as Endangered in May of 2023 (COSEWIC, 2023).

Bats play an important role in the ecosystems they inhabit and their decline in response to threats such as habitat loss, WNS, and wind turbines has concerning implications for both the environment and industry. Their appetite for insects means that bats play a key role in controlling pests in both natural and agricultural contexts (Kunz et al., 2011; Maslo et al., 2022). The presence of bats can reduce forest defoliation by a factor of five (Beilke and O'Keefe, 2023) and it is estimated that insectivorous bats save the United States agricultural industry between $3.7 and $53 billion dollars annually through reduced pesticide application costs (Boyles et al., 2011). If bats continue to decline, this will not only upset the balance between in-

sect pests and natural ecosystems, but also result in additional costs to human food systems.

1.2 Bat Migration

As the majority of North America's bats depend on insects for food, the cooler temperatures and the decline in insect prey that comes with the onset of winter puts them at a loss for resources. North America's insectivorous bat species exhibit two primary strategies to deal with this situation: find a sheltered location to enter hibernation, vastly reducing their energetic requirements, or undergo a longer-distance migration to a location with a milder winter climate (Fleming and Eby, 2003). As is true with the other predominantly tree-roosting species of North America, silver-haired bats fall within the latter category. From studies in the eastern portions of their range, there is evidence that this species travels a north to south migration that can be hundreds or thousands of kilometers in distance (McGuire et al., 2012; Baerwald et al., 2014; Fraser et al., 2017). Understanding of silver-haired bat migrations in their western range is more limited.

In light of the threats that migratory bats face, a better understanding of their spatial movements is key to their conservation (Kunz et al., 2007). Through the identification of summering and wintering grounds, as well as stop-over sites, migratory routes can be determined. These routes can in turn be used to inform decisions around the appropriate siting of wind turbines to limit their impacts on bats, or to identify key habitat for protection (Kunz et al., 2007; Wieringa et al., 2021; Holliday et al., 2023). Furthermore, understanding the primary routes of bat migration could also help indicate where wind turbine curtailment at existing facilities should be implemented for greatest effect. Scientifically informed curtailment of

wind turbine operating times has been shown to significantly reduce impacts on bats (Baerwald and Barclay, 2009; Arnett et al., 2011; Hayes et al., 2019). With deeper knowledge of bat behaviour, the adoption of wind energy need not necessarily come at the cost of migratory bats.

Clarifying the movements of migratory bats can also help us better understand the spread of *Pd* and WNS across North America. While the continent's tree-roosting migratory bats are less susceptible to mortality from WNS, they can carry *Pd* (Bernard et al., 2015; Huebschman et al., 2019). The role migratory bats play as a vector for the disease is unknown, but there is potential for them to move *Pd* over large distances and transfer it to more vulnerable species (Campbell et al., 2022). Information on the spatial movements of migratory bats could help direct WNS detection efforts and the application of future intervention measures that would help protect those bat species most at risk of the disease.

1.3 Studying Bat Movements

The bias to date towards studying silver-haired bat movements east of North America's Continental Divide is not for lack of need, but rather a shortcoming in method. Bats in general are cryptic species, active at night and difficult to capture. Although they are the second-most numerous order of mammals in terms of species and they play such key roles in the ecosystems they inhabit, our knowledge of bat populations is relatively limited (Frick et al., 2020). The techniques available to effectively study bat movements over vast distances have been constrained by technological limitations and the cryptic nature of bats. The radio and GPS transmitters that have become widespread in the study of larger animals remain prohibitively cumbersome for studying small bats over large distances and time frames (Haest

et al., 2021). Marking techniques, such as bands and Passive Integrated Transponders (PIT tags), have long been used to study the movements of small birds. The banding of bats largely ceased in the 1970s out of concern for their well-being (Ellison, 2008). Also, marking methods require close contact with the animal at both its summer and winter locations. This is more feasible for birds, where these summer and winter locations are relatively more well known and a large network of researchers and community scientists exist to collect data. Knowledge of bat summer and winter locations, especially for the more cryptic tree-roosting species, is limited, and the resources necessary to capture the same individual in both locations remains a challenge for the study of bat movements.

The introduction of stable isotope methods to animal migration research provided a new frontier in studying bat movements. Stable isotopes are non-radioactive variants of elements that differ in the number of neutrons that they carry. For example, the most abundant isotope of hydrogen in nature is protium, with one neutron (δ^1H), while the second most abundant isotope is deuterium, with two (δ^2H). The ratio between the abundance of these different isotopes in a measured sample, expressed in per-mil notation (‰), provides information on the sample's stable isotope composition. Stable isotopes of elements contain the same number of protons and electrons, meaning they undergo the same molecular reactions, but the differing number of neutrons results in different molecular masses (Hoefs, 2018). These differing masses result in detectable differences in the way stable isotope ratios are distributed in the environment (Bowen, 2010). These distributions are often dictated by natural climatological and geological processes and express themselves as gradients at the landscape-scale.

The landscape level patterns of stable isotope ratios can be used to trace the origins of migratory bats. Temperate bat species, such as silver-haired bats, undergo a

moult period during the summer, in which they shed and regrow their fur (Fraser et al., 2013). During this moult, the keratin of a bat's hair takes up the isotopic signature of the region in which it is consuming food and water. After growth, this hair becomes largely isotopically inert and the signature remains intact even if the bat moves to another area (Hobson, 1999). As a result, the stable isotope ratios in a migratory bat's hair can indicate the geographic region in which the bat spent the summer months prior to fall migration (Britzke et al., 2009).

Post-moult stable isotope signatures in hair have been used to track the seasonal movements of multiple bat species in North America. The broad-scale geographic gradient of δ^2H has been used to infer the movements of both long-distance migrants, such as the hoary and eastern red bat (Cryan, 2003; Baerwald et al., 2014; Pylant et al., 2014), as well as shorter regional movements by little brown and tri-coloured bats (Sullivan et al., 2012; Fraser et al., 2012). Stable isotope work on silver-haired bats has utilized δ^2H to suggest that within the eastern part of their range, some individuals migrate thousands of kilometers while others remain sedentary (Fraser et al., 2017). With only some exceptions (Cryan, 2003; Cryan et al., 2014), the δ^2H stable isotope work to date has focused on tracking bat movements east of the Continental Divide. In eastern North America, environmental δ^2H ratios follow a relatively smooth gradient of increasing values from south to north, but in the west this pattern is complicated by the more varied topography of the western mountain ranges. δ^2H ratios can be influenced by elevation as well as latitude, and it can be difficult to determine which variable has most strongly influenced a migratory individual's δ^2H signature.

Although δ^2H has been the favoured stable isotope for most bat migration studies, other stable isotopes can contain information about spatial origins. Segers and Broders (2015) used the signatures of δ^{13}C and δ^{15}N to determine that little

brown bats sharing fall swarming sites in Nova Scotia were originating from multiple summer locations. Baerwald et al. (2014) incorporated δ^{13}C and δ^{15}N with δ^{2}H to determine that silver-haired bats killed at wind energy facilities in southwestern Alberta likely originated from areas hundreds of kilometers further north. Still though, these studies were situated east of the Continental Divide. The δ^{13}C and δ^{15}N signatures in bat hair could prove useful in determining the origins of migratory individuals west of the divide. With distributions of δ^{13}C and δ^{15}N varying predictably based on marine influences and changes in elevation (Amundson et al., 2003; Hoefs, 2018), it is likely that these stable isotopes carry strong patterns in western North America.

Through a rigorous method of sampling δ^{2}H, δ^{13}C, and δ^{15}N within the hair of silver-haired bats collected during their summer post-moult period, I have modeled the distributions of these stable isotopes within silver-haired bat hair in western North America. This work represents the first time that these relationships have been explored. By integrating together the unique spatial patterns of each stable isotope under the influence of western North America's varied geography, I have developed a tool that can be used to determine the migratory origins of individuals captured outside of the summer period. I tested this method using silver-haired bats overwintering in coastal southwestern British Columbia and western Washington State, providing the first evidence that bats overwintering in this region likely undergo a longitudinal migration with a large catchment area across southern British Columbia and the Pacific Northwest of the United States. This process shows that stable isotopes can be used to model animal migrations in regions of complex geography, and the resulting information can be used to help plan conservation and mitigation measures to protect migratory bats in the face of multiple threats.

Chapter 2

The Application of Hydrogen, Carbon, and Nitrogen Stable Isotopes to Tracking Silver-haired Bat Migrations in Western North America

2.1 Introduction

Animal migration is driven by a complex suite of factors and serves as proof of the evolutionary adaptability of animal populations in the face of change. Migration's adoption across a broad range of taxa speaks to its utility (Dingle and Drake, 2007). However, migration is an energetically demanding endeavour balancing the costs and benefits of timing, routes, and distances that will be most beneficial to an individual's fitness (Hedenström, 2009; Alves et al., 2013; Brown et al., 2023). There

are often narrow tolerances for unforeseen challenges along the way that can have life or death implications (Bauer et al., 2020; Buechley et al., 2021). Changes in the environment, such as climate change, habitat loss, and the introduction of new barriers such as dams, fences, and wind turbines, are adding additional pressures to migratory populations (Wilcove and Wikelski, 2008). It is important that we understand the dynamics around these movements if we are to conserve migratory animal biodiversity in the face of these growing challenges.

Bats are among the taxa that have taken to migration, although its adoption is not uniform across all species. Temperate insectivorous bats exhibit two primary migration strategies to cope with the declines in temperature and food availability that come with the onset of winter: undergo regional migrations to suitable hibernacula, or undertake longer, continental scale migrations to areas of more favourable winter temperatures. Migratory bats are often tree-roosting species, whose seasonal movements are likely driven by the need to seek out regions where trees can provide sufficient protection from cold winter temperatures (Popa-Lisseanu and Voigt, 2009). For the migratory bats of North America, this often necessitates migrations involving movements of hundreds or thousands of kilometers (Cryan, 2003; Fraser et al., 2017; Wieringa et al., 2021).

The long distance routes of migratory bats are not without their dangers, and this is having a serious impact on their populations. Habitat degradation and insect declines reduce available resources at summer and winter grounds, as well as at stopover sites (Frick et al., 2020), and it has become increasingly apparent that the proliferation of wind energy in North America poses a serious threat to the survival of migratory bat species (Arnett et al., 2016; Frick et al., 2017). As of 2012, an estimated 600,000 bats were killed annually by wind turbines in the United States alone (Hayes, 2013). In an effort to meet renewable energy production targets and

reduce greenhouse gas emissions, the number of wind turbines on the landscape continues to grow (Wiser et al., 2022). This continued growth will put increasing pressure on migratory bat populations unless more is done to mitigate the impacts of wind energy operations.

Understanding the spatial patterns of bat movements is an important step in mitigating the impacts of expanding wind energy development on migratory species (Kunz et al., 2007). However, studying long-distance movements of small, cryptic species remains challenging and many knowledge gaps persist regarding North American bat migrations (Holliday et al., 2023). Closing these gaps is a key component in conserving North America's migratory bats in the face of emergent and persistent threats (Kunz et al., 2007). With the determination of migratory routes and vital overwintering areas, critical habitat can be identified for protection and mitigation measures at turbine sites can be introduced that reduce wind energy's impact on migratory bats.

Silver-haired bats (*Lasionycteris noctivagans*), a predominantly tree-roosting species common across much of Canada and the United States, are among the North American bat species that undergo annual long-distance migrations (Dzal et al., 2009; McGuire et al., 2012). To date, much of the work on silver-haired bat migrations has focused on movements in the portion of North America east of the Rocky Mountains (McGuire et al., 2012; Baerwald et al., 2014; Jonasson and Guglielmo, 2016; Fraser et al., 2017). Less research has been done on the migrations occurring in the western portion of the species' range, although multiple studies have identified a concentration of winter silver-haired bat occurrences in the coastal depression stretching from Portland, Oregon, to north of Vancouver, British Columbia (Izor, 1979; Nagorsen et al., 1993; Cryan, 2003). This area, part of the Georgia Depression and Puget Lowland ecoregions, hereafter referred to as the Georgia-Puget

Lowland, is characterized by moderate temperatures that rarely drop below 0° Celsius in the winter. These mild temperatures appear to provide sufficient foraging opportunities for year-round silver-haired bat occupation of the region (Falxa, 2007). It has been theorized that the silver-haired bats of this area do not undergo migration and that western populations of the species are isolated from those in the east (Cryan, 2003). An alternative that has not been thoroughly examined is that the region's mild winters may make it an attractive migratory destination for silver-haired bats summering across a broader portion of North America.

If silver-haired bats are selecting the Georgia-Puget Lowland as a winter destination for long-distance migrations, this raises a number of conservation concerns. Silver-haired bats account for up to 56% of the turbine-related bat mortalities in North America's Pacific Northwest (Arnett et al., 2008). Wind energy production capacity in Washington and Oregon has grown by over 42% in the last decade and continues to increase (Wiser and Bollinger, 2011; Wiser et al., 2022). If bats are migrating to the Georgia-Puget Lowland, they are potentially passing an expanding gauntlet of turbines along the way. The Lowland itself is also changing. Home to three major metropolitan areas, Vancouver, Seattle, and Portland, the human population of the region continues to grow rapidly (Puget Sound Regional Council, 2022; BCStats, 2022). Forested sites in urban areas can act as refuges for migratory bats (Adams and McGuire, 2022) and development within the region may be impinging on valuable overwintering habitat for silver-haired bats.

Determining the migratory origins of silver-haired bats overwintering in the Georgia-Puget Lowland may also help us better understand threats to other bat species in the region. White-nose syndrome (WNS) and its causative fungus *Pseudogymnoascus destructans* (*Pd*), have now spread to seven counties within this lowland since first being observed in Washington State in 2016 (USFWS, 2023). Although

not heavily impacted by WNS, silver-haired bats are known to carry *Pd* (Bernard et al., 2015; Campbell et al., 2022). As a long-distance migrant, the species could potentially carry *Pd* to regions not yet exposed to the disease. Given the overlap between silver-haired bat winter territory and the current known presence of *Pd*, understanding the species' migratory routes could help direct efforts to monitor the disease's spread.

Stable isotopes have been used to track animal migrations for over forty years (Killingley, 1980) and have provided useful information on the continental movements of bats that would have been difficult to obtain using other methods. Climate and geochemistry dictate the distribution of these stable isotopes in the environment, creating spatially-varied isotopic signatures across the landscape (Bowen, 2010; Hoefs, 2018). Organisms absorb these signatures into their own tissues while consuming local resources (Peterson and Fry, 1987; Hobson et al., 1999). Temperate insectivorous bats undergo a moult in early summer, where newly grown hair absorbs local stable isotope signatures via drinking water and insect prey (Fraser et al., 2013). After this new growth, the keratinous hair becomes metabolically inert, meaning it retains the isotopic signature of its summer location for the remainder of the year (Hobson, 1999). In this way, the stable isotope composition of a bat's hair collected post-migration holds valuable information regarding its geographic origins. Stable isotope signatures have been used to better understand the movements of North America's other migratory bat species (Cryan et al., 2004, 2014; Pylant et al., 2014) and to study the movements of silver-haired bats in their range east of the Rocky Mountains (Baerwald et al., 2014; Fraser et al., 2017).

To date, there has been limited application of stable isotopes to study the movements of silver-haired bats west of North America's Continental Divide. Much of the stable isotope work on bat migration in North America has relied on the use

of hydrogen stable isotope (δ^2H) ratios (Cryan et al., 2004; Britzke et al., 2009; Sullivan et al., 2012; Pylant et al., 2014). In eastern North America, a relatively uninterrupted south to north δ^2H gradient provides a near-ideal pattern for studying latitudinal migrations (Hobson, 1999; Bowen et al., 2005). However, δ^2H patterns can be influenced by changes in elevation, complicating the use of this stable isotope in the mountainous topography of western North America (Cryan et al., 2004). This complication has likely impeded the use of δ^2H in bat migration studies in the west. However, using δ^2H with other stable isotope ratios, such as those of carbon (δ^{13}C) and nitrogen (δ^{15}N), could help overcome the limitations of a single-isotope approach (Cryan et al., 2004; Werner et al., 2020). The spatial distributions of each stable isotope are driven by different environmental processes, meaning different gradients exist on the landscape for each (Hoefs, 2018). The more stable isotopes included in analysis, the more power there is to tap into a geographic location's unique isotopic signature. A multi-isotope approach can provide finer-resolution predictions of a migratory animal's origin and help to overcome the isotopic noise caused by topography's influence on δ^2H.

I implemented a multi-isotope approach to investigate the applicability of using stable isotopes to trace bat migrations in the complicated geography of western North America. To do this, I used δ^2H, δ^{13}C, and δ^{15}N values from silver-haired bats collected across western North America between the onset of summer moult and the beginning of the fall migration. These stable isotope ratios came from hair samples gathered from museum specimens and from published values in previous studies of western silver-haired bat isotopic composition. These values were then modeled against geographic and climatological variables such as latitude, distance from the coast, elevation, and local precipitation to predict reference maps of expected stable isotope ratios, known as isoscapes (Bowen, 2010), for each of the stable isotopes

under investigation. I then used the δ^2H, δ^{13}C, and δ^{15}N values of silver-haired bats overwintering in the Georgia-Puget Lowland to determine their regions of most probable migratory origin on the isoscapes created.

2.2 Methods

With the Georgia-Puget Lowland as the central migratory destination (Figure 2.1), I delineated a study area based on the geographic distribution of available museum specimen and published estimates of silver-haired bat migratory ranges (McGuire et al., 2012; Baerwald et al., 2014; Fraser et al., 2017). This area covered from 55° latitude in the north to 38° latitude in the south, reaching to 103° longitude in the east. This is a region of extreme environmental gradients. Elevation varies from sea level to peaks of up to 4400 meters in the Cascade and Rocky Mountain ranges that run parallel to the Pacific coast. Climate patterns in the area are largely dictated by the influence of the Pacific Ocean in coastal areas and by rain shadow effects of the mountain ranges and valleys to the east. This geography leads to moderate temperatures in coastal areas and more extreme conditions inland, including cold, snowy winters. The result is a landscape with high potential for stable isotope variation.

For stable isotope ratios in bat hair to be representative of the unique environmental conditions in their area of summer residence, it is ideal to sample hair after moult has begun but before the end of the summer residence period. After the summer residence period, the bat may already have begun its migration. I defined the beginning of moult as June 20$^{\text{th}}$, as per Fraser et al. (2017). I used the time prior to peaks in silver-haired bat activity during the late summer and early fall, as identified at nearby acoustic recording stations (Weller 2019; unpublished data; Orville

Dyer personal comm.), to define local completion of the summer residence period. No samples were retained for isoscape development if their collection date occurred after the onset of these activity peaks.

To select museum specimens for sampling, I took a stratified sampling approach. To capture as much geographic variation as possible, I divided the study area into 12 sampling cells and aimed to select an equal number of samples from each cell. These cells were delineated north to south by the 43^{rd}, 47^{th}, and 51^{st} lines of latitude and east to west by the eastern slope of the Coastal/Cascade mountain ranges and the western slope of the Rocky Mountains (Figure 2.1). Each sampling cell was further divided into three strata based on the elevation of the specimens' collection site. I then randomly selected two to three specimens from within each elevation stratum for sampling. If a stratum or sampling cell did not have enough specimens to be fully sampled, I allocated this excess to the nearest cell or stratum with available specimens.

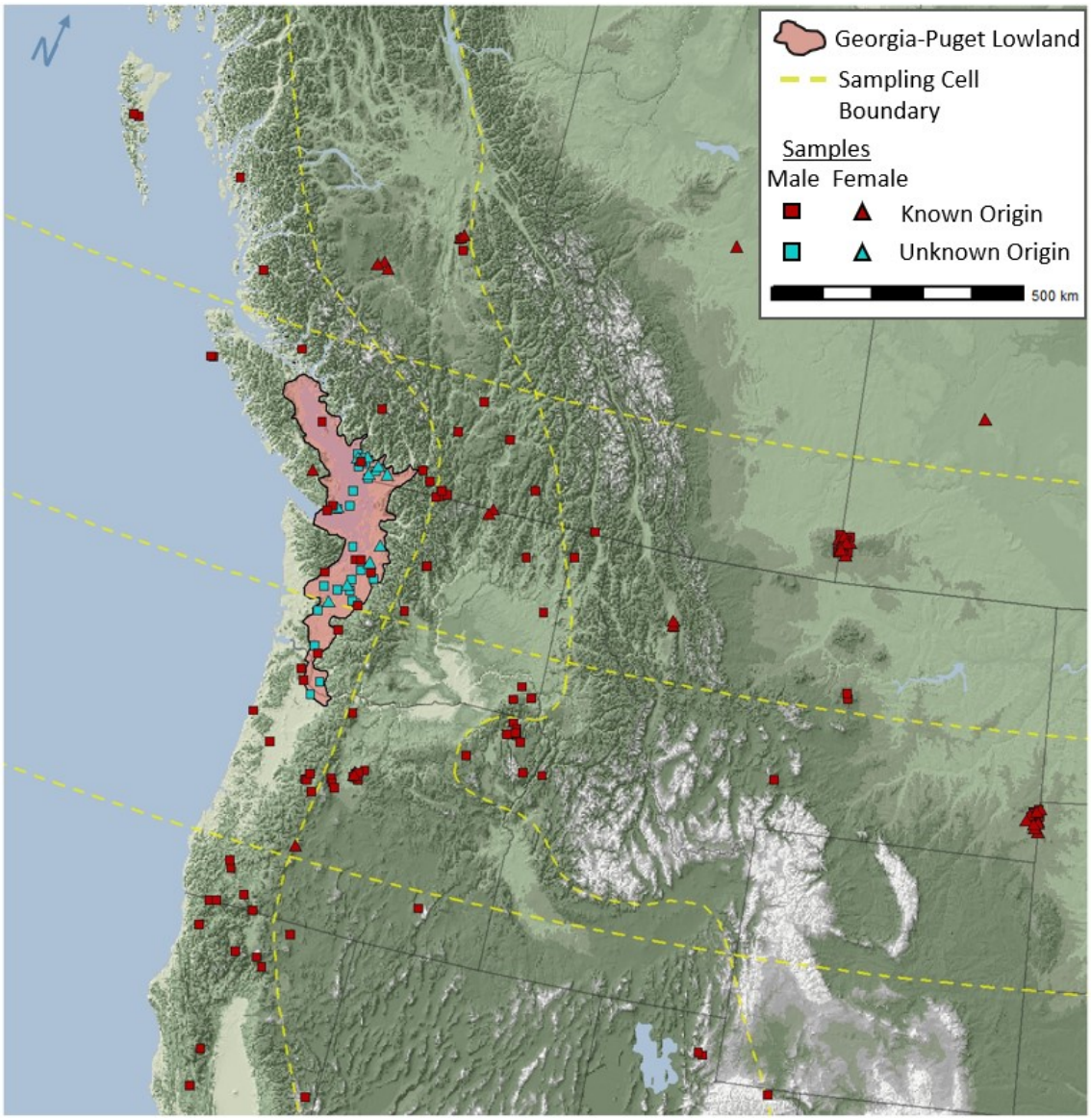

Figure 2.1: Sampling cell boundaries (yellow dashed line) and collection locations (red points) for individual silver-haired bats selected for isoscape development. The boundary of the Georgia-Puget Lowland (shaded in red) and bats identified within for migratory origin tracing (blue points) are also shown. The underlying base map represents an elevation gradient between sea level and 4400 meters above sea level.

I only selected specimens identified as adults, since juveniles and sub-adults may differentially take up environmental stable isotopes (Cryan et al., 2012, 2014; Fraser et al., 2015). I supplemented the samples from museums with stable isotope ratios (δ^2H, δ^{13}C, and δ^{15}N) from adult silver-haired bats published in Fraser 2011 (n

= 21) and Fraser et al. 2013 ($n = 7$) that had been collected after June 20th and before the end of their local residency period. In total, I selected 143 individuals of known origin for isoscape development (Figure 2.1). Due to differences in data availability for some individuals, the number of available samples was reduced to 132 for δ^{13}C and 136 for δ^{15}N.

In addition to the samples identified for isoscape development, I also selected 34 museum specimens, collected outside of the summer moult period for the purpose of determining their summering region. A further two samples were gained from a live individual captured during mist netting and a mortality collected by a member of the British Columbia Community Bat Program, resulting in a total of 36 "unknown origin" candidate individuals, 13 females and 23 males, for origin tracing (Figure 2.1). The collection dates of these individuals ranged from September 24th to February 29th. Only individuals collected within the Georgia-Puget Lowland were selected for origin tracing.

Hair was cut from each individual using clean surgical scissors from the dorsal side of the bat, where moult begins (Fraser et al., 2013). I stored samples in paper envelopes or plastic microcentrifuge tubes until further processing.

To prepare samples for stable isotope analysis, I cleaned each sample by swirling it for two minutes in a solution of 2:1 chloroform:methanol and then leaving it to air dry in a paper envelope for at least 24 hours. All isotope analysis for these samples was completed at Environment and Climate Change Canada's National Hydrology Research Centre (NHRC) Stable Isotope Laboratory in Saskatoon, Saskatchewan. For δ^{2}H analysis, I encapsulated 0.35 mg ($\pm$ 0.05 mg) of hair in silver capsules. NHRC employed a comparative equilibration approach to account for the exchange of keratin hydrogen with ambient vapor (Wassenaar and Hobson, 2003), using reference standards CBS (Caribou hoof, -157‰) and KHS (Kudu horn, -35.3‰) to cali-

brate sample δ^2H (Soto et al., 2017). Samples were thermally converted to gasses at 1450°C, separated chromatographically, and introduced to a ThermoFisher Delta V isotope ratio mass spectrometer (Bremen, Germany – http://www.thermofisher.com). To estimate precision, a subset of samples was duplicated ($n = 10$), with a mean difference between duplicates of ± 2.01‰ (SD = 2.69‰). All δ^2H results are reported as per mil (‰), normalized relative to the Vienna Standard Mean Ocean Water – Standard Light Antarctic Precipitation (VSMOW-SLAP) scale.

I encapsulated 0.5 mg (± 0.07 mg) of sample hair in tin capsules for δ^{13}C and δ^{15}N analysis. These samples were combusted at 1030°C in a Carlo Erba NA1500 elemental analyzer. The resulting N_2 and CO_2 gasses were separated chromatographically and then analyzed by an Elementar Isoprime isotope ratio mass spectrometer (Langenselbold, Germany – http://www.elementar.de). BWBIII keratin (δ^{13}C = -20.18‰, δ^{15}N = 14.31‰) and PRCgel (δ^{13}C = -13.64, δ^{15}N = 5.07‰) standards were used to normalize sample δ^{13}C to Vienna Pee Dee Belemnite (VPDB) and δ^{15}N to atmospheric nitrogen (AIR). Within-run precision from duplicate sample analyses ($n = 10$) was ± 0.09‰ (SD = 0.11‰) for δ^{13}C and ± 0.42‰ (SD = 0.55‰) for δ^{15}N.

Increasing combustion of fossil fuels since the Industrial Revolution has led to a decrease in atmospheric δ^{13}C (Francey et al., 1999), which in turn is reflected in the δ^{13}C of mammalian tissues collected over the same time period (Long et al., 2005). The collection dates of the specimens I selected for analysis ranged from 1896 to 2019, and their δ^{13}C values showed a declining trend with year of collection (r^2 = -0.61, $P < 0.001$). I applied the correction equation defined in Long et al. (2005) to δ^{13}C to get an adjusted $\delta^{13}C_a$ for all further analysis.

I evaluated δ^2H, $\delta^{13}C_a$, and δ^{15}N relationships with climate variables using predicted normals derived from ClimateNA (Wang et al., 2016). Environmental stable

isotope ratios can be influenced by seasonal conditions (Casey and Post, 2011; Metcalfe, 2021). Therefore, I compared the relationship between stable isotope ratios and both the mean annual and mean May to July value of each variable. The May to July period was chosen to represent the environmental conditions directly preceding and during the uptake of environmental stable isotope ratios by the moult process, which occurs from late June to the end of July (Fraser et al., 2017). For climate normals I chose the period from 1961 to 1990, since this represented the tri-decadal period in which the most specimens were collected.

Geographic variables examined included collection site latitude, Euclidean distance from coastline as calculated by the `terra` package (ver. 1.7-65, Hijmans 2023), and elevation from the Global Multi-resolution Terrain Elevation Data 2010 (GMTED2010; Danielson and Gesch 2011). Latitude's relationship with δ^2H is well-documented in other parts of North America (Hobson and Wassenaar, 2008). This relationship is driven by precipitation and evaporation processes (Dansgaard, 1964). For this reason, I also chose to include solar irradiance as a variable, as it factors in latitude, slope, and aspect to potentially provide better resolution data on solar inputs causing evaporation. As δ^{13}C and δ^{15}N ratios are influenced by available moisture, particularly as it pertains to fractionation processes in photosynthesis and evapotranspiration (O'Leary, 1988; Amundson et al., 2003), I explored multiple variables representative of water availability and energy inputs impacting evaporation. These included precipitation, relative humidity, Hargreave's climatic moisture deficit, and elevation. Elevation has a documented relationship with δ^2H (Dansgaard, 1964) and also correlates to moisture drainage and retention along slopes and within valleys (Amundson et al., 2003). Distance from the coast was selected due to known effects of marine environments on δ^2H and δ^{13}C (Lott et al., 2003; Hoefs, 2018) and due to longitudinal patterns in moisture across western North

America driven by consecutive mountain ranges and valleys. This profile of elevation change causes orographic rainfall and rain shadows with the potential to influence δ^{13}C and δ^{15}N distributions. All variables used in the model selection process are summarized in Table 2.1.

Table 2.1: Geographic and climatological variables tested as predictor variables in Generalized Additive Models with δ^{2}H, $\delta^{13}C_a$, and δ^{15}N response variables

Variable	*Source*
Latitude	Specimen Collector
Distance from Coast	R *terra* v1.7-65
Elevation	GMTED2010
Mean Annual Hargreaves Climatic Moisture Deficit	ClimateNA v7.21
Mean Annual Solar Irradiance	ClimateNA v7.21
Mean May to July Solar Irradiance	ClimateNA v7.21
Mean Annual Hargreaves Climatic Moisture Deficit	ClimateNA v7.21
Mean May to July Hargreaves Climatic Moisture Deficit	ClimateNA v7.21
Mean Annual Relative Humidity	ClimateNA v7.21
Mean May to July Relative Humidity	ClimateNA v7.21
Mean Annual Precipitation	ClimateNA v7.21
Mean May to July Precipitation	ClimateNA v7.21

All variable rasters were down-sampled to a 10km resolution to better reflect an estimated home range for silver-haired bats. From these rasters I extracted the covariate values for each sample collection location. I used R (R Core Team, 2023) and ArcGIS 10.8.1 (ESRI, 2020) for all spatial analyses, using the North America Albers Equal Area Conic projection.

For each stable isotope analyzed, I built Generalized Additive Models (GAMs) using a forward step-wise regression approach within the `mgcv` package (ver. 1.8-42, Wood 2011). δ^{2}H, $\delta^{13}C_a$, and δ^{15}N were the respective response variables in each model. I ranked models using Akaike Information Criterion (AIC) model selection

based on minimizing ΔAIC and maximizing model weight (Zuur, 2009). I employed regularization at each step in the process by restricting the spline knots to prevent over-fitting of the smoothing parameters.

In the first step of the model selection process, I looked at single variable models and their respective ΔAIC values to identify the primary large-scale geographic variables (latitude, distance from coast, and solar irradiance) that correlated most strongly with each stable isotope. These became the basis for the models that followed. In the second step I explored integrating finer scale secondary geographic and climate variables that would complement the primary variables to explain local environmental energy inputs and moisture availability driving isotope distributions. These included elevation, mean precipitation, Hargreave's Moisture Deficit, mean relative humidity, and in some cases solar irradiance if neither irradiance nor latitude were identified as the primary correlate. Solar irradiance and latitude correlated strongly (r^2 = -0.77, $P < 0.001$). It was also in the second step that I identified whether the mean annual or mean May to July variable best correlated with the response variable, determining which to include in further steps. In the third and fourth steps I explored incrementally combining secondary variables to identify the model with the lowest ΔAIC and highest model weight.

To create the isoscape surfaces, I first generated a 10km by 10km point grid confined to the geographic extents of the sampled data. I then attributed each of these points with the same climatic and geographic variables used to model the stable isotope relationships. Using the best model for each stable isotope, as identified in the model selection process, I then predicted the stable isotope value and its respective one standard deviation value for each grid point. These grid values were then projected as rasters to create one isoscape for each of δ^2H, $\delta^{13}C_a$, and δ^{15}N.

I input the model surfaces into the continuous-surface assignment framework of the

`assignR` package (ver. 2.2.0, Ma et al. 2020) in R to estimate probability of origin rasters for each unknown-origin individual. `assignR` uses stacked input isoscapes and their 1SD surfaces to compute posterior probabilities of origin at each raster cell, producing a probability of origin surface populated by individual cell probabilities that sum to 1.

To validate the precision and accuracy of the probability of origin surfaces for each unknown-origin individual, I followed the above procedure to produce probability of origin surfaces for each known-origin individual for which there were a complete set of values for δ^2H, $\delta^{13}C_a$, and δ^{15}N ($n = 133$). From each of these probability of origin surfaces I selected the raster cells that represented the upper 10^{th} percentile of predicted sample origin. I then determined whether the true origin of the sample fell within this area, and if it did not, the distance from the true origin to the nearest cell within this 10^{th} percentile of highest predicted origin.

To group the unknown-origin probability surfaces into clusters of like-individuals I used the hierarchical clustering method described by Campbell et al. (2020). I conducted pairwise comparisons between each surface using Schoener's D-metric of niche overlap to characterize likeness (Schoener 1970; as described in Broennimann et al. 2012), producing a symmetric matrix of D values for each pair of unknown-origin individuals. I then input this matrix into the hierarchical clustering tool found in the `pvclust` R package (ver. 2.2-0, Suzuki and Shimodaira 2006) using the "average" method to cluster by correlation distance. This process calculates an Approximately Unbiased (AU) p-value for each identified cluster using multiscale bootstrapping (Suzuki and Shimodaira, 2006). I visually compared the probability of origin surfaces for each individual in the identified clusters to confirm the significance of the clusters identified. To visually summarize the results I created a mean probability of origin raster for each cluster by summing the probability of origin at

each grid cell and dividing this value by the number of individuals in the cluster.

2.3 Results

Environmental relationships were found for each of hydrogen (δ^2H), carbon ($\delta^{13}C_a$), and nitrogen (δ^{15}N). The predominant factor correlating to δ^2H was the mean annual solar irradiance at the location where a bat was collected, while $\delta^{13}C_a$ and δ^{15}N were both most strongly related to longitudinal factors represented by the bat's distance from the Pacific coast. The identification of these trends enabled the creation of isoscapes for each stable isotope. I used these isoscapes and the `assignR` package to trace the probable origins of unknown-origin silver-haired bats, identifying five clusters of bats with similar origin predictions. The majority of the highest-probability origin predictions were located in the interior regions of western North America, to the east of where the bats were collected.

2.3.1 δ^2H Isoscape Development

Mean annual solar irradiance and latitude were both identified as potential primary variables in the δ^2H model selection process. The ultimate best-fitting multivariate model (Table 2.2) integrated mean annual solar irradiance ($P < 0.001$), elevation ($P < 0.01$), and distance from coast ($P = 0.14$). This final model had an adjusted r^2 of 0.29 and explained 32.2% of the deviance in the data.

Table 2.2: Top models and best-fitting individual variables identified during the δ^2H model selection process

Model	Δ *AIC*	*df*	*Weight*
Mean Annual Irradiance + Dist. from Coast + Elev.	0.0	7.7	0.384
Mean Annual Irradiance + Elev.	1.0	4	0.228
Mean Annual Irradiance + Dist. from Coast + Elev. + May-July Precip.	1.3	8.6	0.202
Latitude + Dist. from Coast + Elev. + May-July Rel. Humidity	3.1	9.9	0.081
Latitude + Dist. from Coast + May-July Rel. Humidity	4.0	8.9	0.053
Mean Annual Irradiance + Dist. from Coast + May-July Precip.	5.7	6.8	0.022
Latitude + Dist. from Coast	6.6	5.6	0.013
Mean Annual Irradiance + Dist. from Coast	6.8	5.6	0.013
Latitude	9.7	3	0.003
Mean Annual Irradiance	13.6	3	<0.001
Null	44.2	2	<0.001

The partial effects plot (Figure 2.2) shows the nature of the relationship between each variable and δ^2H values when the other variables in the model are accounted for. A strong positive linear relationship exists between δ^2H and increasing solar irradiance. The curvilinear relationship with the sample's distance from the coast was most significant within the first 200km from the sea, with δ^2H values sharply increasing within the first 100 kilometers before declining over the following 100 kilometers. Increasing elevation had a negative linear relationship with δ^2H.

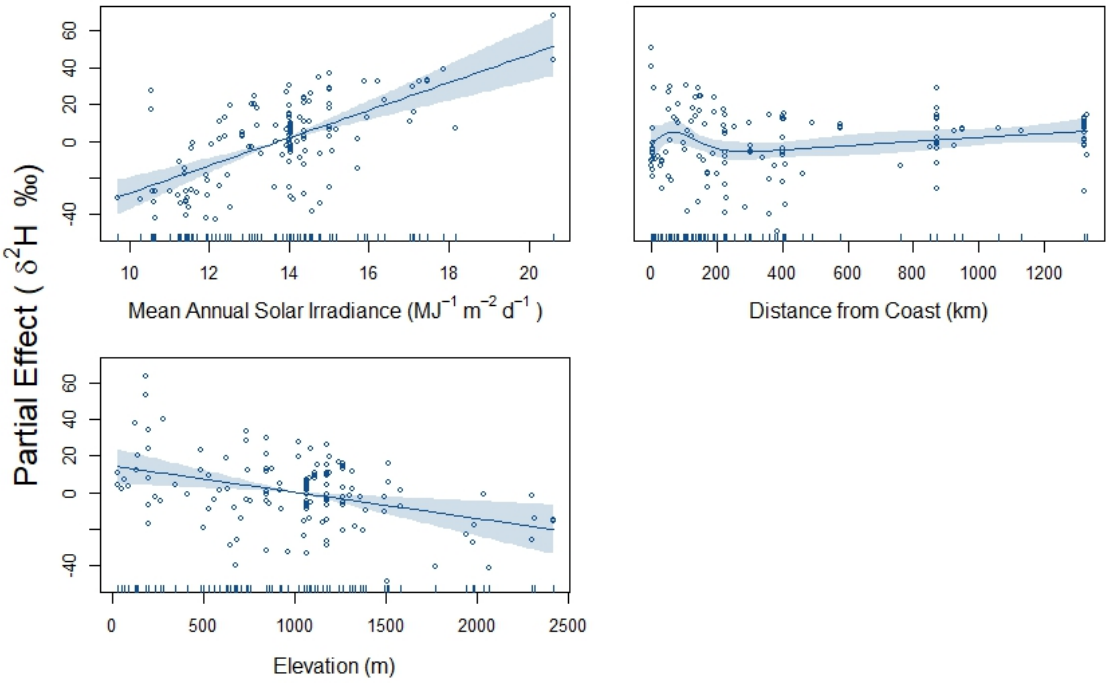

Figure 2.2: Partial Effects Plot for δ^2H Irradiance + Distance from Coast + Elevation model, showing fitted curve against residuals with shaded area representing two standards errors above and below the curve.

The resulting isoscape (Figure 2.3A) shows the north-south gradient for bat hair δ^2H, with values decreasing at higher latitudes. This gradient varies along the significant elevation changes in the study area.

The superimposed δ^2H values for the known-origin samples in Figure 2.3A show the spatial variation in these data, as well as how well the isoscape fits the data. Greater contrast between the sample value and the underlying isoscape surface represent a poorer fit. The isoscape fits these values well across much of the study area. However, higher variation is most notable in the samples collected in Haida Gwaii at the northwest extent of the study area. Model variance, represented by the 1 standard deviation surface (Figure 2.3B), is highest at the geographical extents of the study area, as well as at higher elevations.

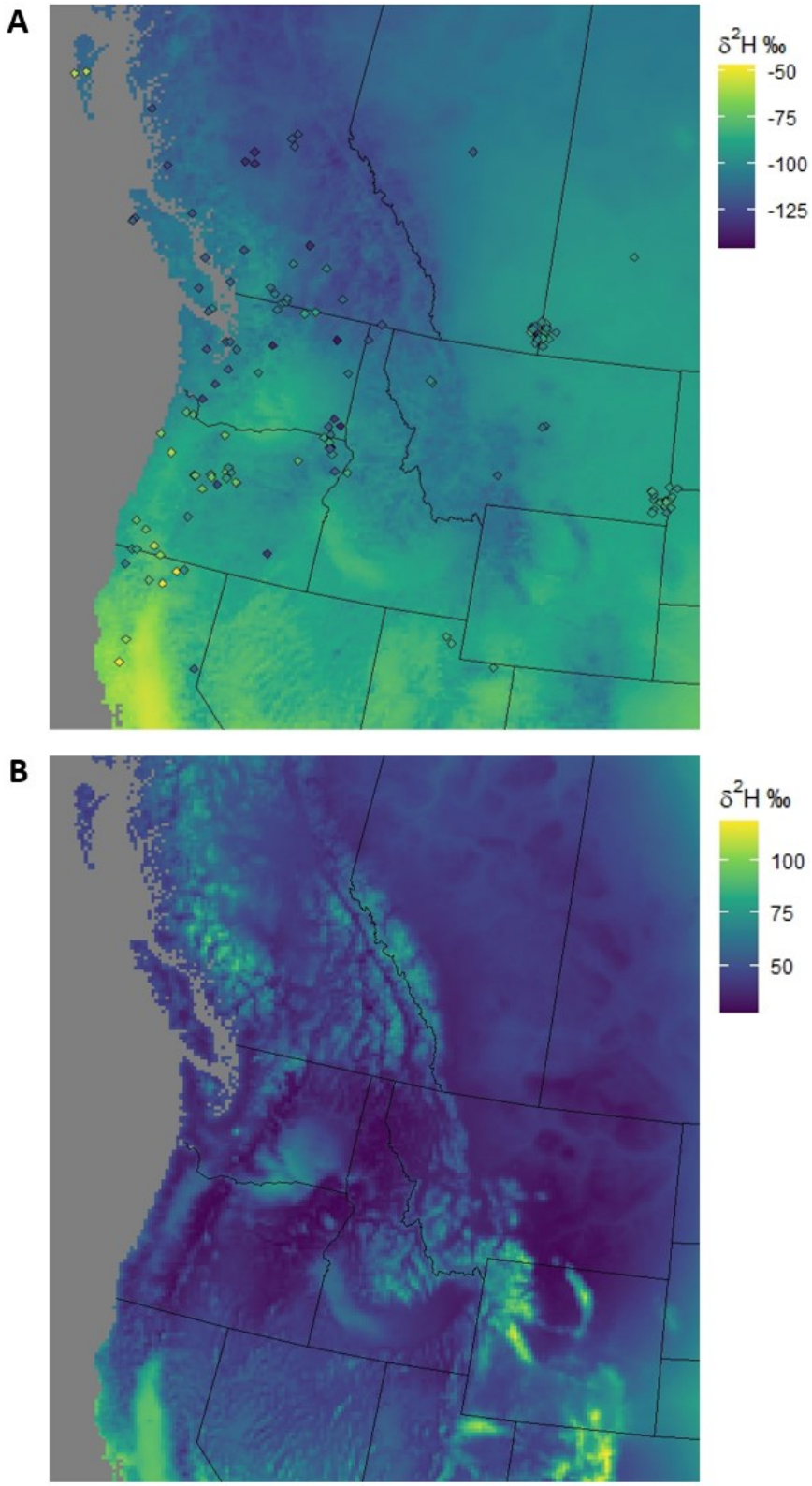

Figure 2.3: (A) Modeled hydrogen isoscape surface with superimposed points showing δ^2H values of the known-origin silver-haired bat samples used to inform the model. With the isoscape and sample values coloured on the same δ^2H scale, contrast between the two shows spatial patterns of model fit. (B) Associated 1 standard deviation surface for the δ^2H isoscape.

2.3.2 $\delta^{13}C_a$ Isoscape Development

Of the univariate models evaluated for their relationship with $\delta^{13}C_a$, distance from the coast had the best fit (Table 2.3). Variables reflecting environmental moisture levels and evaporation, such as mean May to July solar irradiance, mean annual precipitation, and mean annual relative humidity, were prevalent in the best-fitting multivariate models. The model that best described $\delta^{13}C_a$ values in the known-origin samples integrated the collection site's distance from the coast ($P = 0.001$), mean May to July solar irradiance ($P = 0.07$), mean annual relative humidity ($P = 0.07$). This model had an adjusted r^2 of 0.29 and explained 34.2% of the deviance in the data.

Table 2.3: Top models and best-fitting individual variables identified during the $\delta^{13}C_a$ model selection process

Model	Δ *AIC*	*df*	*Weight*
Dist. from Coast + Mean May-July Irrad. + Mean Annual RH	0.0	10.8	0.297
Dist. from Coast + Mean May-July Irrad. + Mean Annual Precip.	0.2	10.3	0.265
Dist. from Coast + Mean May-July Irrad. + Mean Annual RH + Mean Annual Precip.	0.4	11.9	0.244
Dist. from Coast + Mean May-July Irrad. + Mean Annual Precip. + Elev.	1.0	12.4	0.177
Dist. from Coast + Mean Annual RH	6.9	8.3	0.009
Dist. from Coast + Mean May-July Irrad.	7.4	8.8	0.007
Dist. from Coast + Elev.	18.9	6.9	<0.001
Dist. from Coast	19.6	5.9	<0.001
Dist. from Coast + Mean Annual Precip.	19.9	6.9	<0.001
Null	47.5	2	<0.001

The partial effects plot (Figure 2.4) shows that $\delta^{13}C_a$ values were lowest at the coast, sharply increasing within the first 100 kilometers from the ocean before dipping in the 150 to 300 kilometer zone before increasing again. The effect of solar irradiance only influenced $\delta^{13}C_a$ at lower values of irradiance, causing an increase

in $\delta^{13}C_a$. The relationship between $\delta^{13}C_a$ and mean annual relative humidity was linear and negative.

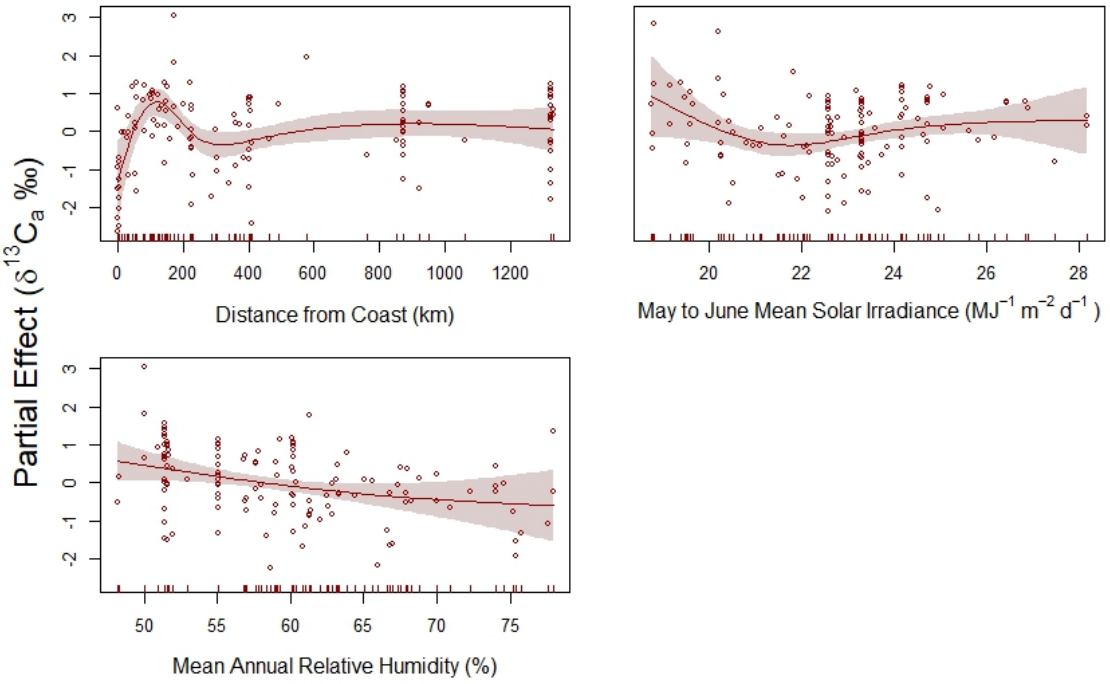

Figure 2.4: Partial Effects Plot for $\delta^{13}C_a$ Distance from Coast + Irradiance + Precipitation model, showing fitted curve against residuals with shaded area representing two standards errors above and below the curve.

The $\delta^{13}C_a$ isoscape (Figure 2.5A) displays patterns of longitudinal banding reflective of the topography of the study area. Areas along the coast and higher elevations of the Canadian Rocky Mountains are depleted of $\delta^{13}C_a$ relative to lower elevation interior regions. Observation of the superimposed known-origin sample values reveals no apparent patterns in deviation from the modeled isoscape.

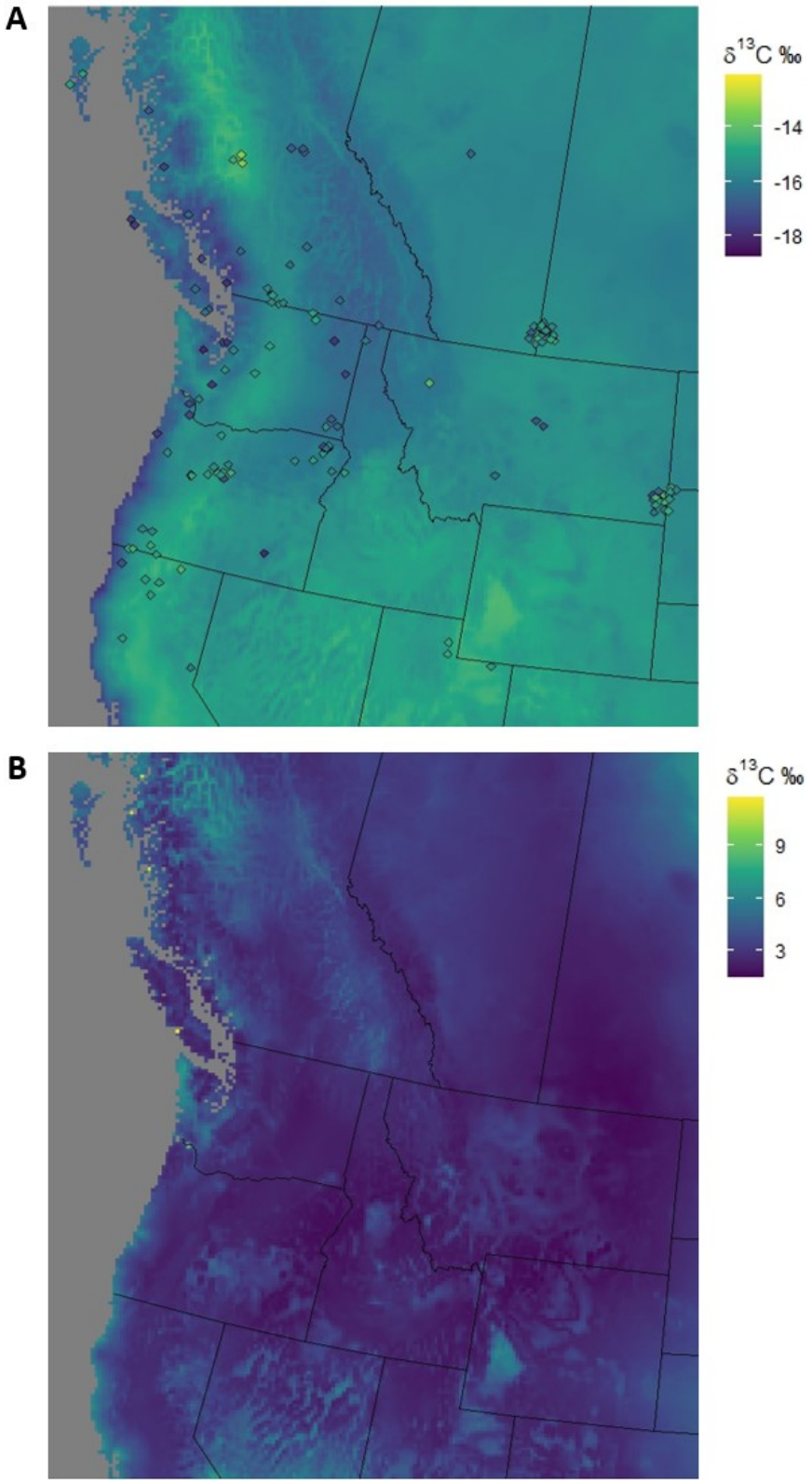

Figure 2.5: (A) Modeled carbon isoscape surface with superimposed points showing $\delta^{13}C_a$ values of the known-origin silver-haired bat samples used to inform the model. With the isoscape and sample values coloured on the same $\delta^{13}C$ scale, contrast between the two shows spatial patterns of model fit. (B) Associated 1 standard deviation surface for the $\delta^{13}C$ isoscape.

Across most of the $\delta^{13}C_a$ isoscape, standard deviation (Figure 2.5B) varied by $< 6‰$. Higher uncertainty exists in the model at more elevated areas of British Columbia and particularly in higher elevation areas of the southern portion of the study area.

2.3.3 δ^{15}N Isoscape Development

Within the single variable nitrogen models (Table 2.4), distance from the coast best explained the δ^{15}N patterns ($P < 0.001$). δ^{15}N was lower adjacent to the coast and rose with distance (Figure 2.6). Incorporating mean annual precipitation ($P < 0.001$) further refined this model (deviance explained = 62.8%), with declining δ^{15}N as regions became wetter. However, this trend reversed at around 1000 millimeters of rain per year and δ^{15}N increased logistically at higher precipitation values. Incorporation of elevation ($P = 0.02$) into the model further increased the deviance explained to 63.8% and visual inspection of the partial effects plot (Figure 2.6) revealed an enriching factor at elevations below 500 meters. The adjusted r^2 of the model incorporating distance from coast, mean annual precipitation, and site elevation was 0.62.

Table 2.4: Top models and best-fitting individual variables identified during the δ^{15}N model selection process

Model	Δ *AIC*	*df*	*Weight*
Dist. from Coast + Mean Annual Precip. + Elev.	0.0	9.8	0.972
Dist. from Coast	8.7	5	0.012
Dist. from Coast + Mean Annual Precip.	10.4	6	0.005
Dist. from Coast + Elev.	10.7	6	0.005
Dist. from Coast + Mean Annual RH	10.7	6	0.005
Dist. from Coast + Elev. + Mean Annual RH	13.4	7.1	0.001
Null	122.4	2	<0.001

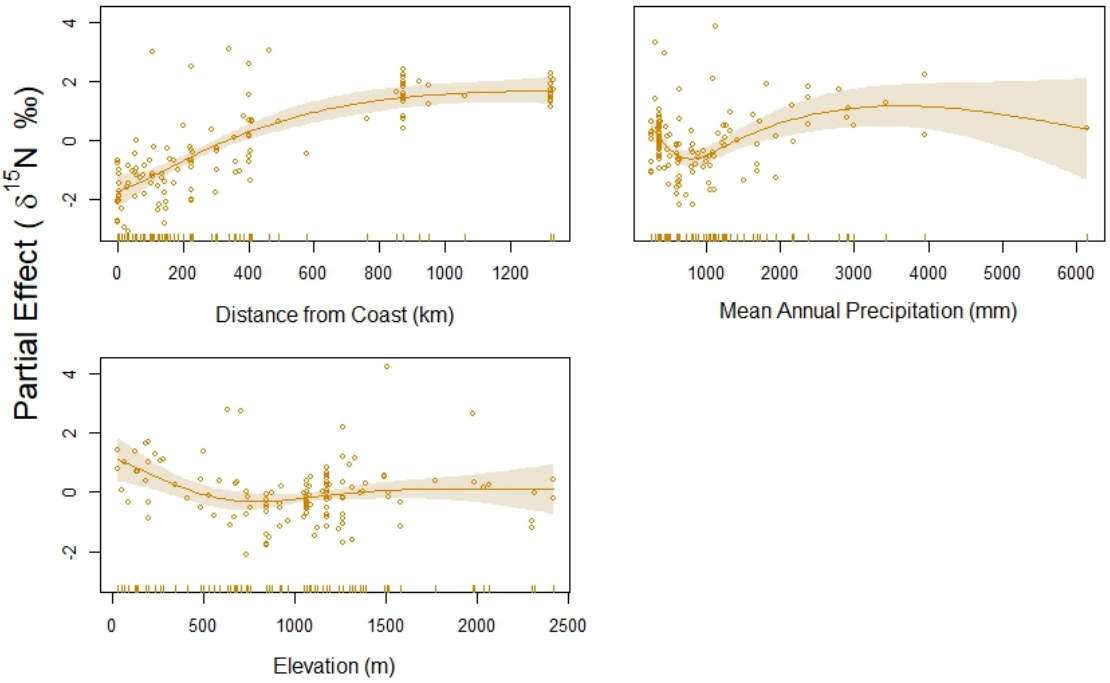

Figure 2.6: Partial Effects Plot for δ^{15}N Distance from Coast + Mean Annual Precipitation + Elevation model, showing fitted curve against residuals with shaded area representing two standards errors above and below the curve.

The δ^{15}N isoscape (Figure 2.7A) is dominated by a longitudinal gradient, with more enriched values being found towards the eastern portion of the study area. The influence of the mean annual precipitation and elevation variables is reflected in the variations to this gradient, which largely follow the patterns of topography for the region. The superimposed δ^{15}N values of the samples used to inform this model fit these patterns well, although more extreme outliers are visible. This is particularly apparent in some samples from interior regions of southern British Columbia, eastern Washington, and northeastern Oregon that contrast with the underlying isoscape.

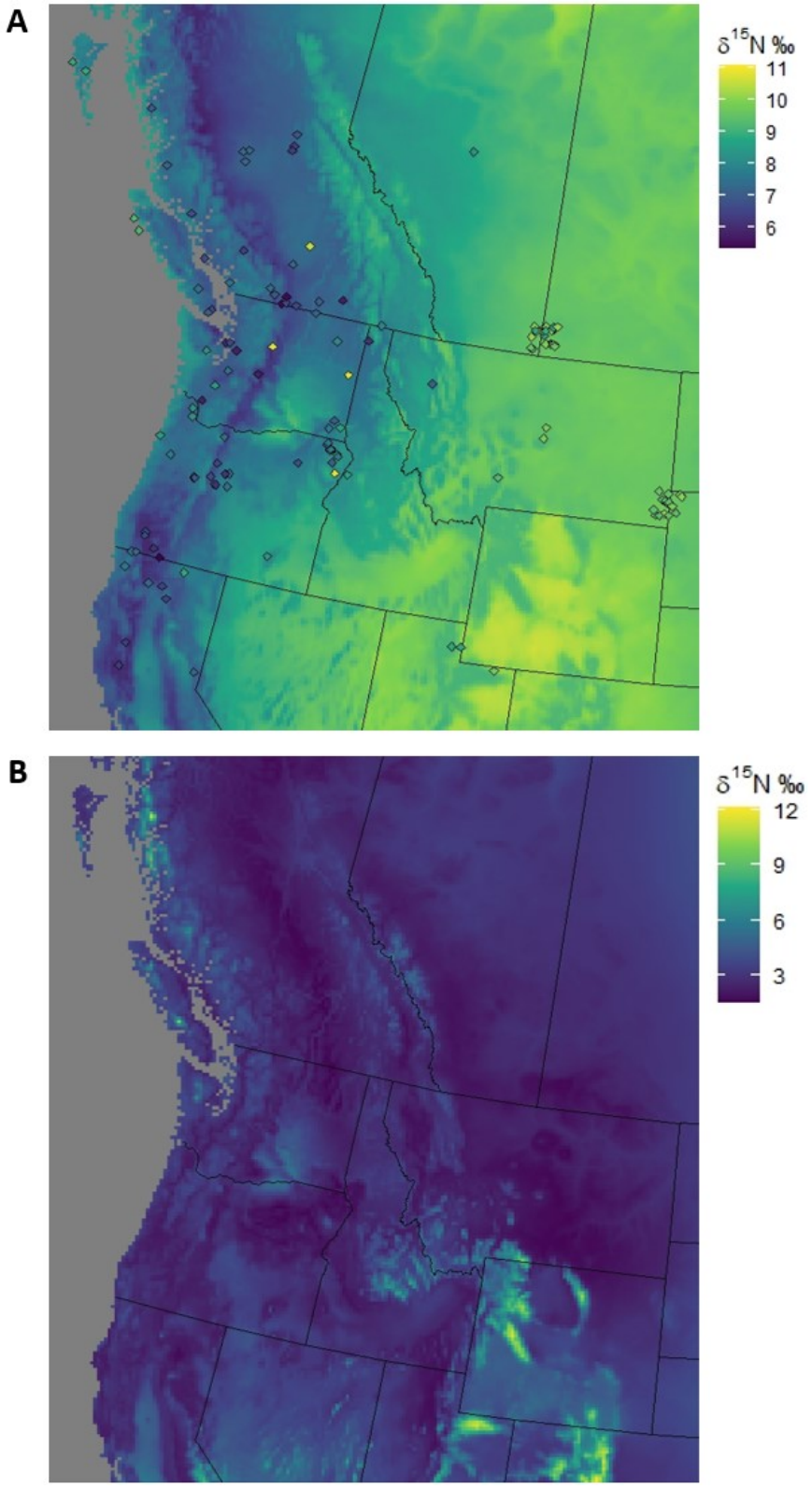

Figure 2.7: (A) Modeled nitrogen isoscape surface with superimposed points showing δ^{15}N values of the known-origin silver-haired bat samples used to inform the model. With the isoscape and sample values coloured on the same δ^{15}N scale, contrast between the two shows spatial patterns of model fit. (B) Associated 1 standard deviation surface for the δ^{15}N isoscape.

The standard deviation surface for δ^{15}N (Figure 2.7B) mostly varies between 2 and 4‰, although higher regions of model variance are visible in the central Columbia Basin of Washington, the northern coast of British Columbia, and the southeastern portion of the study area.

2.3.4 Geographic Assignment of Unknown-Origin Samples

The `assignR` continuous-surface assignment framework generated probability of origin rasters for each of the 36 unknown-origin individuals. Using hierarchical cluster analysis of these rasters, the cluster dendrogram (Figure 2.8) of like individuals was created. Based on visual confirmation of the rasters within each cluster, I identified five clusters ranging from 2 to 17 individual bats of unknown origin.

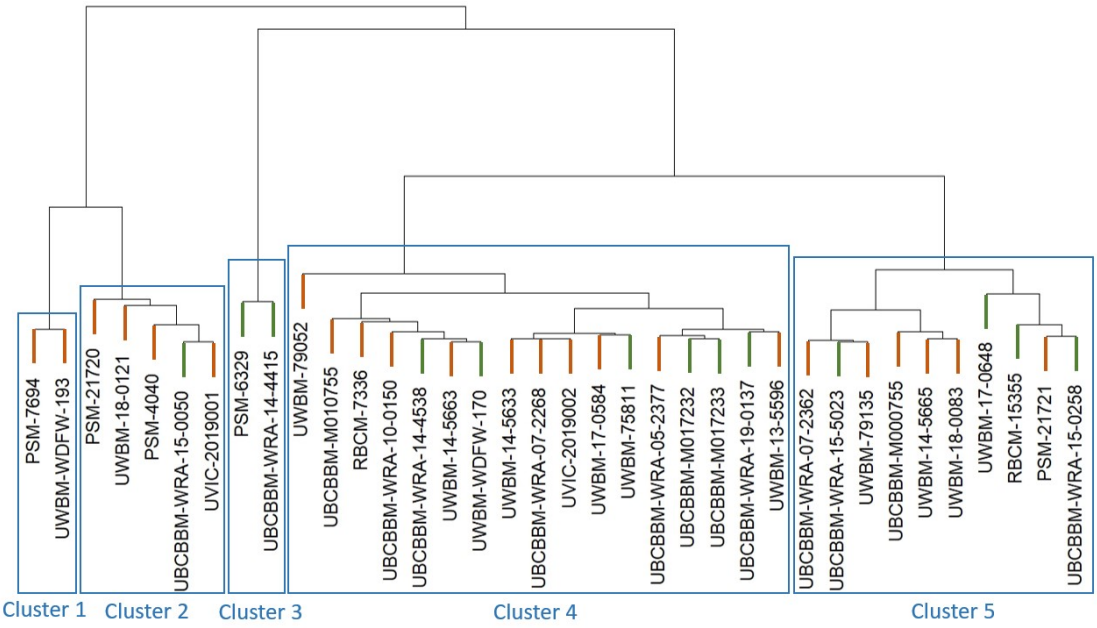

Figure 2.8: Cluster dendrogram for silver-haired bats overwintering in the Georgia-Puget Lowland. Male individuals are represented by an orange branch while females are green.

Figure 2.9 shows the mean probability of origin surfaces for the clusters identified by the hierarchical cluster analysis. The highest predicted probability of origin for Cluster 1 ($n = 2$) occurred along the eastern slopes of the Cascade Mountain

Range, stretching from southern British Columbia in the north to as far south as northern California. Cluster 2 ($n = 5$) also shows higher probabilities directly east of the Cascade Mountains, but also shows high likelihoods of originating in British Columbia's Central Interior and the Blue Mountains of northeastern Oregon. Cluster 4 represents the largest proportion of bats ($n = 17$) and has a similar signature to Cluster 2, minus the high probabilities in the eastern Cascades. Cluster 3 ($n = 2$) and Cluster 5 ($n = 10$) show the most distinct difference between their location of collection and their predicted origin, with high probabilities of origin ranging from within the Rocky Mountains to as far east as western Montana.

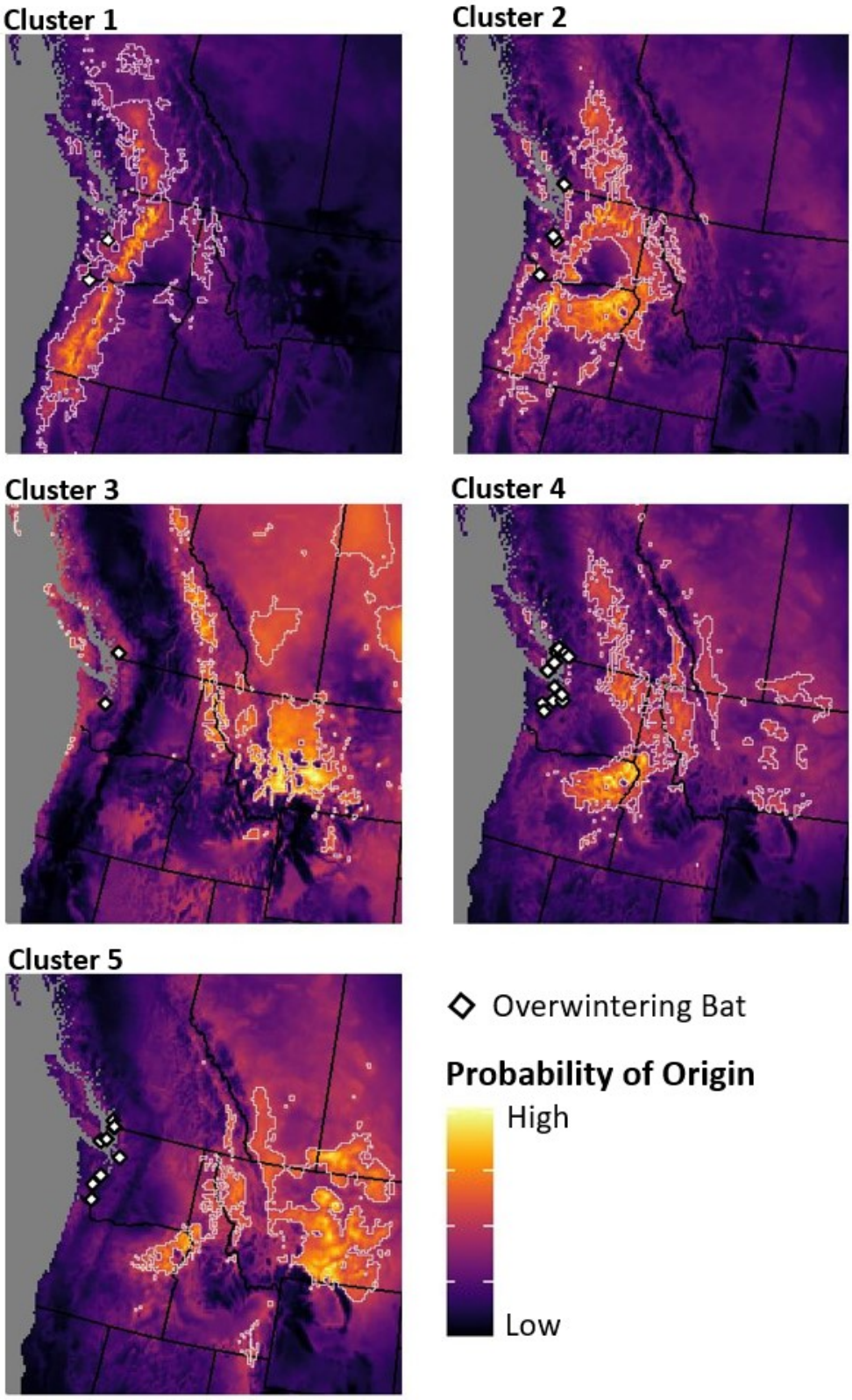

Figure 2.9: Mean probability of origin surfaces for each cluster of silver-haired bats used for origin-tracing. Each pixel in the surface is assigned a probability of origin ranging from low (black) to high (bright yellow). White diamonds show the location of collection for each bat in the cluster, and white lines show the bounds of each cluster's highest 10^{th} percentile of probability of origin.

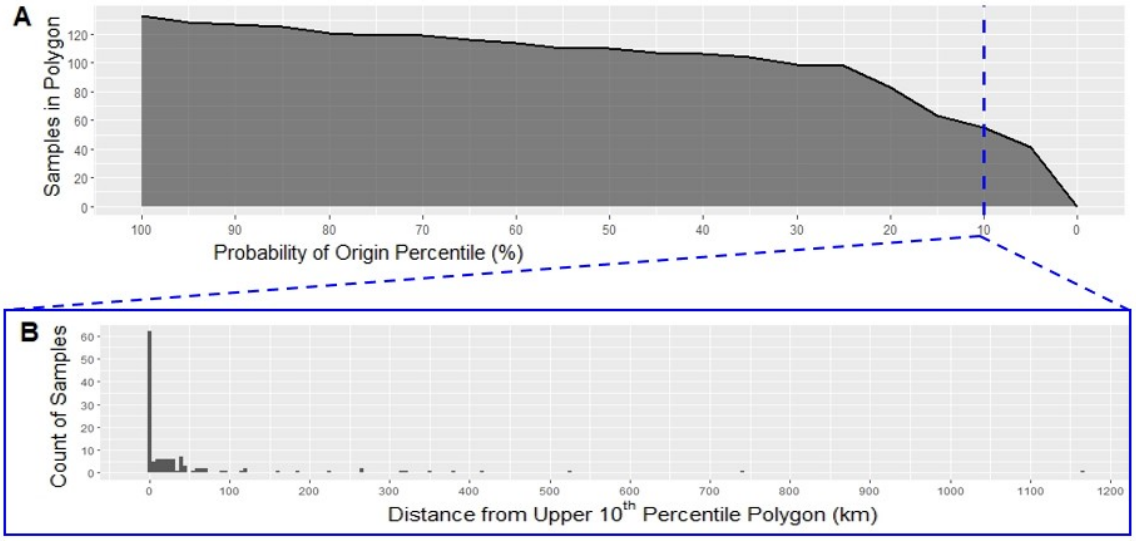

Figure 2.10: (A) The number of known-origin silver-haired bats falling within the boundaries of polygons representing varying probability of origin percentiles, as predicted by AssignR. Values to the left of the Probablity of Origin Percentile scale represent larger predicted polygons of origin and therefore lower precision. The blue dotted line marks the upper 10^{th} percentile, chosen here to represent a high level of precision and shown in Figure 2.9 by the white boundaries. (B) Given this 10^{th} percentile level of precision, the distance between each known-origin silver-haired bat's collection location and the nearest boundary of its predicted area of origin is shown.

Figure 2.10 provides insight into the accuracy and precision of the probability of origin predictions. These are the results of running the known-origin silver-haired bats through the same prediction process used for the unknown-origin bats. Figure 2.10A shows the number of known-origin bat samples whose true origins fell within their respective predicted origin polygons at varying probability percentiles. Larger probability of origin percentiles represent correspondingly larger polygons of predicted origin, and are therefore less precise. The 100^{th} percentile polygon encompasses the entire study area and therefore logically captures all 133 samples. At a higher level of precision and therefore a smaller polygon, denoted in 2.10A by the blue line at the upper 10^{th} percentile, 55 known-origin samples fell within their respective 10^{th} percentile polygons. Therefore, 41.4% of known-origin samples were accurately predicted at this level of precision. Selecting this high precision 10^{th} per-

centile threshold, Figure 2.10B shows how far the true origin of each sample was from the nearest boundary of its predicted upper 10^{th} percentile polygon. For those bats whose true origin did not fall within their predicted 10^{th} percentile polygons, the median distance from their known origin to the nearest boundary of their polygon was 30.8 kilometers. Of the samples that were not accurately predicted within their upper 10^{th} percentile polygon, sixty-two (79.5%) were within 100 kilometers or less of their respective polygon.

2.4 Discussion

With this thesis, I aimed to both test the viability of stable isotopes as a tool for studying bat migrations in the complex geography of western North America and to apply this method to study the movements of silver-haired bats overwintering in the Georgia-Puget Lowland. Through the application of Generalized Additive Models (GAMs) I was able to identify predominant geographical and climatological factors influencing the hydrogen (δ^2H), carbon (δ^{13}C), and nitrogen (δ^{15}N) stable isotope ratios of silver-haired bats across western North America. The bat-hair stable isotope distribution maps (isoscapes) created from this modelling process enabled the successful identification of general patterns of migratory origin for silver-haired bats overwintering in the Georgia-Puget Lowland, providing the first evidence of longitudinal east-west migration in this species. The evaluation of stable isotopes as geographic tracers in the context of western North America and the ecological implications of these results are expanded upon below.

2.4.1 Stable Isotopes as Geographic Tracers

I identified significant geographic patterns in each of the stable isotopes incorporated into the models for isoscape development. The δ^2H ratios in silver-haired bat hair carried a strong latitudinal signal while the ratios of δ^{13}C and δ^{15}N revealed longitudinal patterns driven by changes in coastal influences, topography, and moisture availability. The use of multiple stable isotopes driven by different processes greatly improved the resolution of geographic assignments for migratory bats of unknown origin.

A strong relationship between bat hair stable isotope ratios of hydrogen (δ^2H) and latitude is known and well-documented in movement studies in eastern North America (Britzke et al., 2009; Fraser et al., 2012, 2017). Latitude is strongly correlated with solar irradiance, which I found to be the strongest predictor of δ^2H in silver-haired bats. Even in the more varied geography in the western portion of North America, latitudinal factors continue to have a strong correlation with δ^2H distributions in the environment. Similarly, these results also corroborate the presence of the negative relationship between δ^2H and elevation (Dansgaard, 1964), and the smaller variance in δ^2H for bats collected adjacent to the coast may be reflective of the fact that marine areas are uniform in their δ^2H ratios (Hoefs, 2018).

The longitudinal profile of the $\delta^{13}C_a$ relationship with distance from coast shows varied influences. The low values for samples collected at the coast may be reflective of marine sources of carbon being more depleted in δ^{13}C (Hoefs, 2018). The changes in $\delta^{13}C_a$ moving away from the coast mirrors the profile of the major mountain ranges and valleys in the study area. These geographical features and their related rain shadow effects impact the plant community composition of these regions, another factor known to affect δ^{13}C distributions (Schulze et al., 1998; Bowling et al., 2002; Metcalfe, 2021). For plants following the C_3 pathway, the dom-

inant photosynthetic pathway in western North America (Still et al., 2003; Suits et al., 2005), there is a tendency for $\delta^{13}C$ to increase with declining moisture in the environment (Stewart et al., 1995; McCarroll and Pawellek, 2001; Bowling et al., 2002). This pattern transfers to higher trophic levels (Popa-Lisseanu et al., 2015), and likewise the $\delta^{13}C_a$ values in silver-haired bat samples showed this same negative relationship with higher available moisture, as reflected by lower levels of solar irradiance and relative humidity (Figure 2.4).

The prevalent pattern for $\delta^{15}N$ in the known-origin samples was a longitudinal gradient increasing further in-land, reflected by the distance from coast variable. A similar longitudinal gradient for $\delta^{15}N$ in western North America was predicted by Amundson et al. (2003) in their work on global nitrogen stable isotope distributions. $\delta^{15}N$ declined with increasing mean annual precipitation below 1000 mm/year, a trend noted in other studies (Amundson et al., 2003; Luo et al., 2018), however it then rose again with more extreme local precipitation. This pattern may be reflective of an environmental shift to denitrification when precipitation crosses a threshold, resulting in $\delta^{15}N$ enrichment (Hoefs, 2018). Overall, moisture gradients appeared to be a major factor in the distribution of $\delta^{15}N$ within the study area.

The models of $\delta^{2}H$, $\delta^{13}C_a$, and $\delta^{15}N$ respectively explained 32.2%, 34.2%, and 63.8% of the deviance in the data. The utility of GAMs to describe non-linear relationships greatly increased these models' ability to account for the effects of spatial and climatic variables across their full range of values. This in turn enables finer-resolution isoscapes more reflective of stable isotope variation at smaller scales, resulting in more precise predictions of origin for migratory individuals. This precision would not have been possible using strictly linear methods of regression and modeling, and these results highlight the value that additive modeling can bring to isoscape development.

A number of factors could be contributing to the deviance not explained by the models. The 10 kilometer grid selected for the climate variables may not capture specific variations in habitat that could be influencing isotopic conditions at smaller scales. Even isotopic signatures from samples collected at the same location can be highly variable. These levels of within-site intraspecific variation are not uncommon (Voigt et al., 2015; Popa-Lisseanu et al., 2015), and could be a result of differences in prey selection, foraging habitat, or isotopic tissue assimilation by individual bats (Cryan et al., 2012). Additionally, the use of climate normals based on a specific period, in this case 1961 to 1990, to model the isotopic conditions for bats collected over a much broader period (1896 to 2019) does not capture interannual fluctuations such as El Niño/Niña and the North Pacific Oscillation. While long-term records of these events exist, factoring them into these models and the resulting predictions of origin was determined to be too complex for this study as it would require developing unique isoscapes for each explicit time period of climate variation.

These results highlight the importance of using multiple stable isotopes in migration studies involving areas of high geographic variability such as western North America. Even in this study area, with its highly variable topography, δ^2H serves as a strong indicator of latitudinal origin. However, beyond being subject to immediate coastal influences, δ^2H does not vary strongly along a longitudinal orientation. Therefore, δ^2H alone is limited in what it can provide in areas where there are potential longitudinal migrations occurring. Conveniently, the longitudinal moisture gradients caused by the north-south oriented mountain ranges of western North America are reflected in the patterns of δ^{13}C and δ^{15}N observed here. These results show that within the context of western North America, δ^{13}C and δ^{15}N complement δ^2H well in migratory origin tracing studies by providing a longitudinal signal.

The integration of these three stable isotopes allows for more refined predictions of probable origin. The same is likely true for other regions of the world where stable isotopes have not been applied to study animal migrations due to their complex geography.

While the combination of δ^2H, δ^{13}C, and δ^{15}N worked well together to rule out large areas of potential origin, the identified areas of probable origin remain relatively large. Further work is needed to improve the precision and confidence of predicted origins. The models were limited by the availability of bats collected at the more extreme geographical limits of the study area. This included areas of higher elevation and latitude. This explains the higher variance in the 1 standard deviation surfaces in those areas (Figures 2.3B, 2.5B, 2.7B). Dedicated sample collection targeting these areas would help to more clearly define the bat hair-stable isotope relationships in these regions.

As has been shown here, integrating multiple stable isotopes driven by differing environmental processes can serve to increase the precision of origin assignments for migratory bats. Additional tracers could further refine the geographic assignments found here. Sulphur (δ^{34}S) stable isotope distributions are known to be influenced by sea salt aerosol deposition and the presence of isotopically heavy marine sulphates in coastal food systems, resulting in strong marine versus inland signatures (Zazzo et al., 2011; Bataille et al., 2021). The inclusion of δ^{34}S could help further clarify the terrestrial origins of bats overwintering in the coastal Georgia-Puget Lowland. Additionally, strontium (^{87}Sr/^{86}Sr) ratios are driven by the geological age and lithology of bedrock and, though costly to analyze, show promise for improving the precision of isotope-based geographic assignments (Bataille and Bowen, 2012; Bataille et al., 2020; Reich et al., 2021). The integration of Species Distribution Models (SDMs) can further refine predictions of origin, given that suitable

habitat is heterogeneous across the landscape (Cryan et al., 2014; Wieringa et al., 2020, 2023). The incorporation of contaminants or trace elements has also been suggested for use in studying bat movements, although these techniques may be better suited to areas of high pollution or shorter regional movements (Brewer et al., 2021). However, some work has been done to show that broad-scale spatial variation of atmospheric mercury deposition is reflected in bat tissues (Chételat et al., 2018) and that continental bat migration can be studied when multiple trace elements are applied (Wieringa et al., 2020). The use of δ^2H, δ^{13}C, and δ^{15}N in this study acts a promising start to the implementation of intrinsic markers on bat migration research west of North America's Continental Divide.

2.4.2 Ecological Implications

The majority of silver-haired bats of unknown-origin that were collected while overwintering in the Georgia-Puget Lowland showed isotopic evidence of having spent their summer in a different location. These results indicate that this region serves as a migratory catch basin for a wide area of western North America. Some individuals showed a high probability of originating from as far away as western Alberta and Montana, suggesting that the Rocky Mountains are not an obstacle to the westward migration of silver-haired bats. Most of the individuals studied had isotopic signatures indicative of areas east of where they wintered, namely the dry lowland interior and mountainous regions of southeastern British Columbia, eastern Washington, and northern Oregon and Idaho. Relative to the mild, short winters of the Georgia-Puget Lowland, these areas experience long, cold winters that force bats to enter torpor for extended periods of time to ensure winter survival. The choices an animal must make around migration are a cost-benefit endeavour, with the option that leads to the greatest benefit at the least cost often meaning the difference

between success and failure (Hedenström, 2009). By selecting a longitudinal east-west migration route, silver-haired bats in western North America can expend less energy than would be required to reach similar climates via a north-south migration route. While the distance between the Georgia-Puget Lowland and the areas of most likely origin identified here range between about 400 and 500 kilometers, a flight southward to similar winter climates would take upwards of 600 to 900 kilometers. Cryan et al. (2014) found evidence of a similar longitudinal migration in North American hoary bats (*Lasiurus cinereus*) and Norquay et al. (2013) observed longitudinal movements between summer roosts and winter hibernacula in little brown bats. In other regions, such longitudinal migration routes have been observed in birds (Areta and Bodrati, 2008; Davenport et al., 2012; Lees, 2016) and east-west migrations could become more common with global climate change (Dufour et al., 2021). The mild, short duration winters of the Georgia-Puget Lowland likely serve as an attractive migratory destination for silver-haired bats seeking to conserve their energetic costs.

For silver-haired bats traveling this east-west route, the proliferation of wind turbines in the region poses a serious threat. In North America, wind turbines were estimated to kill between 148,000 and 308,000 silver-haired bats between 2000 and 2011 (Arnett and Baerwald, 2013) and in Washington and Oregon up to 56% of turbine-related bat mortalities are silver-haired bats (Arnett et al., 2008). Wind energy capacity in Washington and Oregon has grown by over 42% between 2011 and 2022 and is projected to continue growing (Wiser and Bollinger, 2011; Wiser et al., 2022). The majority of this expansion has occurred along the Oregon-Washington border in the Columbia River Valley (Figure 2.11; USGS 2023). This valley sits between the Georgia-Puget Lowland and interior summering grounds identified in this study. It has been hypothesized that bats favour linear features such as

river valleys for their migrations (Furmankiewicz and Kucharska, 2009; Wieringa et al., 2021; Micalizzi et al., 2023), and therefore wind turbines situated along the Columbia River Valley and other low mountain passes pose a serious threat to silver-haired bats undergoing seasonal movements. The number of bats killed at wind farms can be reduced through both turbine curtailment (Baerwald et al., 2009; Arnett et al., 2011) and the use of deterrents (Arnett et al., 2013; Weaver et al., 2020). These methods can reduce mortalities by as much as 93% (Arnett et al., 2011). However, the implementation of federal mitigation guidelines is voluntary in the United States (USFWS, 2012) and even in jurisdictions where regulations exist, their level of implementation and enforcement varies (Arnett et al., 2016). Given current declines in populations of migratory bats (Frick et al., 2017; COSEWIC, 2023), every effort must be made to protect their populations. My results emphasize the need for scientifically-informed and well-enforced strategies to lessen the impact of wind energy development on migratory bats in the Pacific Northwest region. These measures should include stringent curtailment at existing facilities and a ban on new turbines within the passes most likely acting as a funnel for migratory bats moving across the mountain ranges of western North America to overwinter on the Pacific coast.

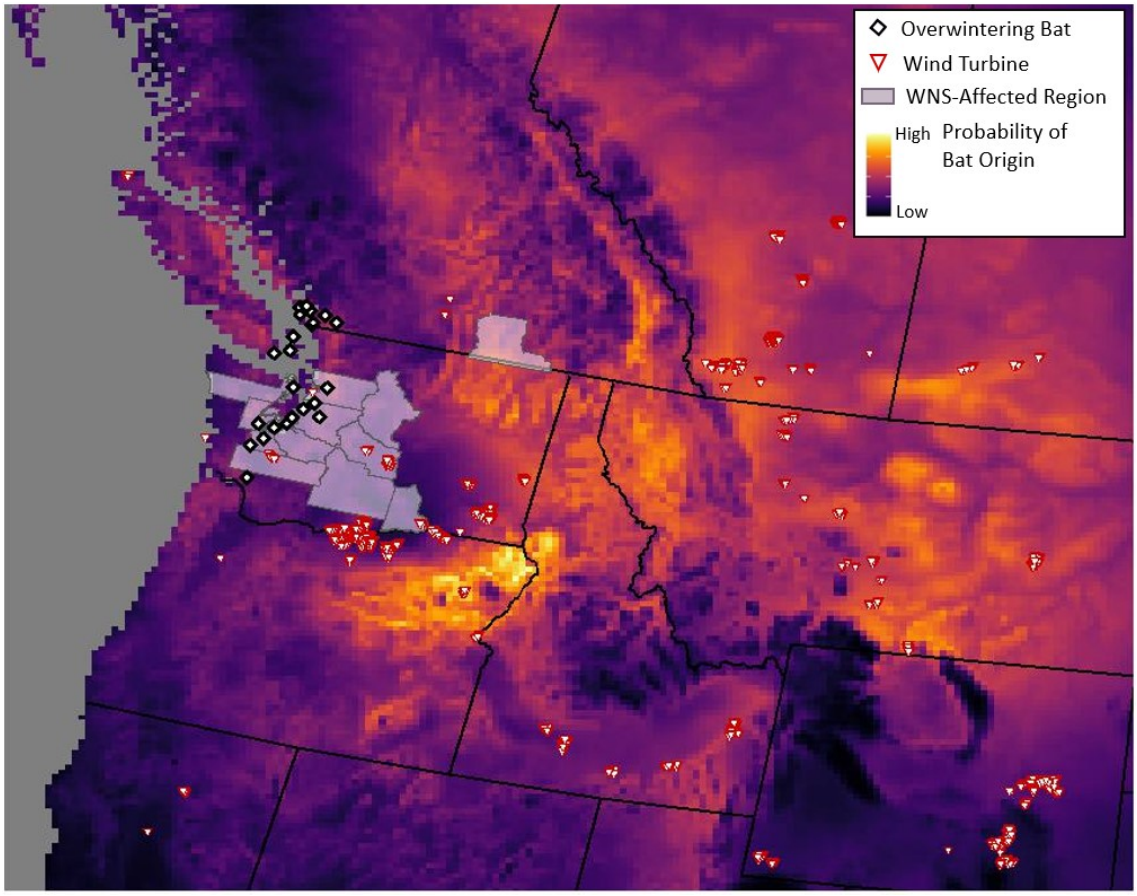

Figure 2.11: Mean probability of origin surface for overwintering silver-haired bats (white diamonds) within clusters 3, 4 and 5 ($n = 29$), showing areas of high probability of migratory origin in yellow. Active wind turbines (red-outlined triangles) and regions of *Pd* or WNS detection are also shown.

This evidence of migratory movement between the Georgia-Puget Lowland and interior regions to the east may help predict the spread of threats to other bat species, as well. The presence of white-nose syndrome (WNS) and *Pseudogymnoascus destructans* (*Pd*), the fungus responsible for WNS, has now been found in seven counties within this lowland, a further four counties directly to the east, and one regional district of southern British Columbia (Figure 2.11; USFWS 2023). While silver-haired bats have not been heavily impacted by WNS, they are known to carry *Pd* (Bernard et al., 2015; Campbell et al., 2022). To date, WNS and *Pd* have not been widely observed in the areas identified in this study as summering grounds for

bats overwintering on the coast. Silver-haired bats could come into contact with *Pd* while overwintering in the Georgia-Puget Lowland and transfer it to areas not yet exposed to the fungus during spring migration, thus acting as a vector for the disease. Understanding these migratory pathways can assist with predicting the next locations of WNS emergence and help direct monitoring for the disease's spread. A number of promising treatments for this disease are under development (Cheng et al., 2017; Palmer et al., 2018; Rocke et al., 2019), but rapid response to its emergence may be key to successful intervention (Grider et al., 2022). If silver-haired bats are acting as a vector for *Pd*, my results suggest that we should expect the disease to continue to spread eastward.

The isotopic evidence provided in this chapter shows that the Georgia-Puget Lowland likely acts as overwintering habitat for silver-haired bats from a broad region of western North America. The Georgia-Puget Lowland is becoming increasingly urbanized and the habitat within it progressively more fragmented. These findings highlight the need to further refine our knowledge of the habitat most valuable to overwintering silver-haired bats within these coastal areas, and ensure that this high-value habitat is protected. As threats to migratory bats persist and their numbers continue to decline, the identification and protection of overwintering grounds will play an important role in their conservation.

2.5 Conclusion

While the latitudinal pattern of δ^2H found in the hair of western silver-haired bats further supports this stable isotope as a powerful tool for studying animal migrations, my integration of δ^{13}C and δ^{15}N stable isotopes and the application of Generalized Additive Models to determine their spatial relationships was essential to pre-

dicting the migratory origins of silver-haired bats in western North America. δ^{13}C and δ^{15}N carry a longitudinal pattern of distribution in western North America and GAMs can capture finer-scale variations in isotopic influences, both factors enabling higher-resolution predictions of origin for migratory individuals. This work represents the first time these methods have been combined to study the movements of a migratory bat west of the Continental Divide, and provide novel evidence that silver-haired bats overwintering in the Georgia-Puget Lowland undergo a longitudinal migration from interior regions of the continent. This information should be used to inform conservation planning for bats, including identifying critical habitat and flyways for migratory species and implementing impact mitigation strategies for the expanding wind energy sector in western North America.

Chapter 3

General Conclusions

My goal with this thesis was to develop a method of employing stable isotopes to reveal information on the migratory movements of silver-haired bats in western North America, and to apply this tool to determine the origins of individuals overwintering in the Georgia-Puget Lowland. Mountainous and coastal areas have long been considered a challenge for studies aiming to trace migratory origins using stable isotopes (Hobson, 1999). The high geographic variation of western North America creates a complex isotopic landscape that is challenging to characterize at finer scales, given the multitude of factors that can influence local stable isotope ratios. To be applicable to migration studies, a clear understanding is necessary of how these variations are reflected in the stable isotope ratios of bats consuming resources within their environment. I approached this challenge by systematically identifying bats that had been collected across the broad range of geography representative of western North America, and sampling their hair for multiple stable isotopes during the period when the hair best represents the isotopic signature of that area. I then modeled the hairs' δ^2H, δ^{13}C, and δ^{15}N values against geographic and climatological variables to develop generalized isoscapes. I used these isoscapes

to determine probable regions of migratory origin for bats overwintering in the Georgia-Puget Lowland.

Although samples were limited in some areas, each of the stable isotopes used in this study revealed patterns of distribution suitable to the continental scale of silver-haired bat migrations. The predominantly latitudinal pattern of δ^2H, complimented by the primarily longitudinal distributions of δ^{13}C and δ^{15}N, as well as smaller scale influences of elevation and climate on these stable isotopes, mean that δ^2H, δ^{13}C, and δ^{15}N work well together to provide insight into the general summer origins of silver-haired bats in western North America. This work shows that with careful selection of both the samples and stable isotopes used, along with thoughtful consideration of the underlying geographic and climatological processes that drive their ratio distributions, stable isotopes are an effective tool for studying the movements of migratory bats in western North America.

This thesis provides the first empirical evidence that silver-haired bats overwintering in the Georgia-Puget Lowland are conducting an east-west migration from interior regions of western North America. My results reveal that silver-haired bats migrating to the Georgia-Puget Lowland likely originate from a broad area of southeastern British Columbia, eastern Washington, and northern Oregon and Idaho. Not only does this identify the direction of migration, but also probable pathways between these locations can be inferred. If migrating silver-haired bats are choosing the least energetically costly path of migration (Hedenström, 2009) or using river valleys to guide their migrations (Furmankiewicz and Kucharska, 2009; Wieringa et al., 2021), then the major rivers cutting through the Coastal and Cascade Mountain Ranges, namely the Fraser and Columbia Rivers, may serve as primary migration corridors for this species. More research is required to determine the precise routes silver-haired bats are taking between these locations, but these

initial results already provide useful information for bat conservation. Threats to bats in this region are numerous, including loss of habitat, the spread of white-nose syndrome, and expanding wind energy development.

These results highlight the importance of the Georgia-Puget Lowland as a migratory destination for silver-haired bats. Overwintering locations are critical habitat for bats (Environment Canada, 2015) and given the rapidly growing human population within the Georgia-Puget Lowland, it is important that bats be considered year-round when planning development and identifying natural areas to be protected. Silver-haired bats are active in this region throughout the winter (Falxa, 2007), and acoustic and radio-tracking methods can be used to identify their specific winter habitat requirements within the Georgia-Puget Lowland. At the finest scale, radio telemetry can be used to identify what structures are being used as winter roosts and we can ensure that these are preserved.

With white-nose syndrome being present within the Georgia-Puget Lowland, and silver-haired bats being known carriers of its causative fungus *Pd*, this new information about their movements can contribute to predictions of the disease's potential spread. While it is imperative that the search for WNS and *Pd* continue across the continent, my results can help direct monitoring for the disease given that resources for such monitoring are often limited. If silver-haired bats are vectors for the disease, their longitudinal migrations from the Georgia-Puget Lowland could be carrying the disease to areas of southeastern British Columbia and the northeastern Pacific Northwest that have yet to be exposed to WNS. With potential interventions to WNS impacts on the horizon, locating pockets of the disease is key to early detection and rapid response.

Most importantly, given the drastic impact that wind energy development is having on migratory bats (Kunz et al., 2007; Arnett and Baerwald, 2013; Frick et al.,

2017), these results highlight the necessity for scientifically-informed mitigation strategies for wind turbine operations within the Pacific Northwest. Wind energy is a key component in the necessary move away from fossil fuel-derived energy and this shift need not come at the expense of the continent's migratory bats. Wind turbine curtailment strategies, informed by knowledge of bat ecology, can help reduce the industry's impact on declining bat populations (Baerwald et al., 2009; Arnett et al., 2011; Hayes et al., 2019). The longitudinal pathways between the Georgia-Puget Lowland and the summering grounds I have identified are an area of expanding wind energy development, and my findings provide a clear case for curtailment of existing facilities and restrictions on new ones along these connections. More broadly, these results prove that stable isotopes can be useful tools to track animal migrations in areas of complex topography such as western North America. Key to such efforts is developing species-specific isoscapes derived from tissue samples of individuals collected across a broad range of geographic and climate conditions to capture the natural variation in the landscape. High environmental variation also increases the need to incorporate multiple stable isotopes into such studies, as complementary isotopes influenced by different factors can help refine predictions of probable origin. The methods employed here are applicable across much of the world and to any migratory species that undergoes a known temporal exchange of tissues. Stable isotopes are especially helpful where study species are cryptic or resources for recapture or tracking are limited. This is especially true for bats, and stable isotopes have a key place among the methods needed to reveal their migratory behaviour. That being said, it is important to recognize the limitations and strengths of the stable isotope method so it can be used appropriately. Stable isotope ratios in the environment are subject to many influences and our current knowledge of these influences, as well as our ability to model them, mean

that they are more chainsaw than scalpel: they are a tool for tackling problems at broad scales. While our ability to refine the predicted resolution of stable isotope distributions in the environment will no doubt improve over time, stable isotopes are most effective at identifying broad scale patterns in animal movements.

While bats have proven capable of adapting to an incredibly wide range of ecosystems, the rapid changes they are experiencing from factors such as habitat loss, advancing diseases such as white-nose syndrome, and the expansion of wind energy development are having a significant impact on their populations around the globe. Better understanding key components of bat ecology and behaviour, such as migration, is an important step in identifying threats to their populations and developing conservation strategies. Where other methods such as radio telemetry or banding may be limited in range or resource-intensive in terms of capture effort, stable isotopes offer an efficient method for determining broad-scale patterns in bat migration. Time may be running short to gather the information necessary to effectively protect bat species from extinction. The efficiency advantages provided by stable isotopes should be leveraged to identify landscape- and regional-scale patterns in bat movements and direct finer scale methods such as radio telemetry, where needed, for greatest success. In this sense, each method can be played to its strengths, optimizing the necessary information gathering to identify acute threats and protect migratory bats.

Appendix A

Stable Isotope Compositions of Samples

Sample ID	Use	Sex	Collection Date	Longitude	Latitude	$\delta^{13}C$	$\delta^{15}N$	$\delta^{2}H$	$\delta^{18}O$	$\delta^{13}C_a$	Source
c1-08	Iso.	Female	20/07/2008	-109.8666	49.54996	-22.7	10.2	-99	NA	-14.46	Fraser 2011
c38-08	Iso.	Female	26/07/2008	-109.8666	49.54996	-24.5	9.4	-101	NA	-16.26	Fraser 2011
c11-08	Iso.	Female	01/08/2008	-109.8666	49.54996	-23.9	8.8	-100	NA	-15.66	Fraser 2011
c23-08	Iso.	Female	01/08/2008	-109.8666	49.54996	-22.8	10.5	-70	NA	-14.56	Fraser 2011
c31-08	Iso.	Female	01/08/2008	-109.8666	49.54996	-23.9	10.1	-125	NA	-15.66	Fraser 2011
CL1-09	Iso.	Female	20/07/2009	-109.8666	49.54996	-24.2	9.5	-103	NA	-15.92	Fraser 2011
CL2-09	Iso.	Female	20/07/2009	-109.8666	49.54996	-24.2	9.4	-103	NA	-15.92	Fraser 2011
CL4-09	Iso.	Female	22/07/2009	-109.8666	49.54996	NA	9.6	-101	NA	NA	Fraser 2011
CL10-09	Iso.	Female	28/07/2009	-109.8666	49.54996	-23.8	9.9	-100	NA	-15.52	Fraser 2011
CL9-09	Iso.	Female	28/07/2009	-109.8666	49.54996	-23.9	8.9	-103	NA	-15.62	Fraser 2011
CL11-09	Iso.	Female	29/07/2009	-109.8666	49.54996	-24.3	9.7	-101	NA	-16.02	Fraser 2011
CL12-09	Iso.	Female	29/07/2009	-109.8666	49.54996	-23.9	10	-101	NA	-15.62	Fraser 2011
CL14-09	Iso.	Female	01/08/2009	-109.8666	49.54996	-23.2	9.6	-97	NA	-14.92	Fraser 2011
c37-08	Iso.	Male	31/07/2008	-109.8666	49.54996	-23.9	10.2	-99	NA	-15.66	Fraser 2011
c10-08	Iso.	Male	01/08/2008	-109.8666	49.54996	-23.6	10.3	-111	NA	-15.36	Fraser 2011
CL3-09	Iso.	Male	21/07/2009	-109.8666	49.54996	-23.4	9.9	-81	NA	-15.12	Fraser 2011
CL5-09	Iso.	Male	22/07/2009	-109.8666	49.54996	-23.7	9.9	-92	NA	-15.42	Fraser 2011
CL6-09	Iso.	Male	22/07/2009	-109.8666	49.54996	-25.2	8.5	-100	NA	-16.92	Fraser 2011
CL7-09	Iso.	Male	22/07/2009	-109.8666	49.54996	-23	10.1	-86	NA	-14.72	Fraser 2011
CL13-09	Iso.	Male	01/08/2009	-109.8666	49.54996	-22.9	8.8	-87	NA	-14.62	Fraser 2011
CL15-09	Iso.	Male	02/08/2009	-109.8666	49.54996	-23.4	9.5	-85	NA	-15.12	Fraser 2011
CMN-10156	Iso.	Male	10/08/1929	-116.559985	49.089977	-23.28	7.97	-120.81	8.07	-16.56	Canadian Museum of Nature
CMN-14625	Iso.	Male	21/08/1936	-125.533333	50.666667	-23.01	6.72	-120.81	8.78	-16.24	Canadian Museum of Nature
CMN-15101	Iso.	Male	28/06/1937	-127.231	51.659	-24.15	7.24	-123.48	7.91	-17.37	Canadian Museum of Nature
CMN-2501	Iso.	Male	10/08/1915	-124.416667	49.666667	-23.99	6.68	-117.54	7.81	-17.35	Canadian Museum of Nature
CMN-3401	Excl.	Male	30/08/1918	-118.05	52.883333	-24.36	6.58	-146.16	8.41	-17.71	Canadian Museum of Nature
CMN-6661	Iso.	Female	19/07/1926	-114.3	53.933333	-23.31	8.26	-118.29	7.55	-16.61	Canadian Museum of Nature
CRCM-46-224	Iso.	Male	21/07/1946	-117.6775	46.25056	-22.37	7.63	-114.47	8.16	-15.518	Charles R. Conner Museum
CRCM-54-183	Iso.	Male	07/07/1954	-117.238	46.33	-23.53	8.69	-136.9	6.08	-16.58	Charles R. Conner Museum
IMNH-7368	Excl.	Male	24/08/1964	-112.456655	42.87961	-21.36	7.42	-95.38	9.32	-14.27	Idaho Museum of Natural History
KU-123124	Iso.	Male	14/07/1970	-104.18079	45.65166	-24.15	9.14	-124.32	7.07	-16.96	KU Natural History Museum
KU-123125	Iso.	Male	15/07/1970	-104.18079	45.65166	-24.56	9.33	-92.02	7.86	-17.37	KU Natural History Museum
KU-123126	Iso.	Male	16/07/1970	-104.18079	45.65166	-23.77	10.26	-99.71	8.38	-16.58	KU Natural History Museum
KU-123127	Iso.	Female	16/07/1970	-104.18079	45.65166	-22.09	10.12	-86.42	7.47	-14.90	KU Natural History Museum
KU-123129	Iso.	Female	16/07/1970	-104.18079	45.65166	-21.71	9.57	-87.38	7.52	-14.52	KU Natural History Museum

KU-123133	Iso.	Female	16/07/1970	-104.18079	45.65166	-23.08	9.36	-98.42	8.03	-15.89	KU Natural History Museum
KU-123134	Iso.	Female	17/07/1970	-104.18079	45.65166	-21.62	9.72	-85.25	7.96	-14.43	KU Natural History Museum
KU-123135	Iso.	Male	17/07/1970	-104.18079	45.65166	-23.3	9.42	-96.93	8.07	-16.11	KU Natural History Museum
KU-123137	Iso.	Female	17/07/1970	-104.18079	45.65166	-21.8	9.52	-89.24	8.27	-14.61	KU Natural History Museum
KU-123140	Iso.	Female	17/07/1970	-104.18079	45.65166	-21.87	9.46	-84.98	7.86	-14.68	KU Natural History Museum
KU-123141	Iso.	Female	17/07/1970	-104.18079	45.65166	-21.52	9.45	-84.42	7.55	-14.33	KU Natural History Museum
KU-123143	Iso.	Female	17/07/1970	-104.18079	45.65166	-22.34	9.51	-89.88	7.08	-15.15	KU Natural History Museum
KU-123148	Iso.	Female	17/07/1970	-104.18079	45.65166	-22.49	9.29	-88.3	7.12	-15.30	KU Natural History Museum
KU-123153	Iso.	Male	17/07/1970	-104.18079	45.65166	-23.01	9.43	-83.99	7.38	-15.82	KU Natural History Museum
KU-123155	Iso.	Male	17/07/1970	-104.18079	45.65166	-22.42	9.88	-87.88	7.74	-15.23	KU Natural History Museum
KU-123158	Iso.	Male	20/07/1970	-104.18079	45.65166	-23.77	9.44	-95.82	8.52	-16.58	KU Natural History Museum
KU-123159	Iso.	Male	24/07/1970	-104.09836	45.6227	-22.22	9.74	-102.91	7.38	-15.03	KU Natural History Museum
KU-123161	Iso.	Male	24/07/1970	-104.09836	45.6227	-22.35	10.04	-81.35	8.56	-15.16	KU Natural History Museum
KU-123615	Iso.	Male	11/07/1970	-110.80105	45.79554	-23.35	9.25	-112.51	6.92	-16.16	KU Natural History Museum
KU-135251	Iso.	Male	17/07/1968	-123.195	47.425	-25.25	8.27	-122.16	6.12	-18.10	KU Natural History Museum
KU-169690	Iso.	Male	06/07/1978	-121.556531	41.825367	-21.66	8.82	-96.5	11.23	-14.32	KU Natural History Museum
KU-33774	Excl.	Female	21/08/1949	-111.2454	44.6622	-22.74	8.5	-115.62	9.65	-15.85	KU Natural History Museum
KU-33775	Excl.	Female	21/08/1949	-111.2454	44.6622	-23.5	8.47	-116.62	12.16	-16.61	KU Natural History Museum
KU-33776	Excl.	Female	21/08/1949	-111.2454	44.6622	-22.83	8.27	-118.75	9.42	-15.94	KU Natural History Museum
KU-33777	Excl.	Male	21/08/1949	-111.2454	44.6622	-23.45	8.45	-109.09	10.89	-16.56	KU Natural History Museum
KU-33778	Excl.	Female	21/08/1949	-111.2454	44.6622	-22.93	8.67	-99.98	9.86	-16.04	KU Natural History Museum
KU-33779	Excl.	Male	21/08/1949	-111.2454	44.6622	-23.07	8.6	-110.67	9.19	-16.18	KU Natural History Museum
KU-33780	Excl.	Female	21/08/1949	-111.2454	44.6622	-24.96	8.94	-116.72	9.49	-18.07	KU Natural History Museum
KU-33781	Excl.	Female	21/08/1949	-111.2454	44.6622	-22.87	9.14	-111.32	7.7	-15.98	KU Natural History Museum
KU-33784	Excl.	Female	22/08/1949	-111.2454	44.6622	-23.4	8.71	-119.2	9.89	-16.51	KU Natural History Museum
KU-33787	Excl.	Male	22/08/1949	-111.2454	44.6622	-23.18	8.5	-114.3	10.16	-16.29	KU Natural History Museum
KU-33788	Excl.	Female	22/08/1949	-111.2454	44.6622	-23.58	9.18	-108.95	7.79	-16.69	KU Natural History Museum
KU-33790	Excl.	Male	23/08/1949	-111.2454	44.6622	-23.38	8.7	-100.58	8.8	-16.49	KU Natural History Museum
KU-45596	Iso.	Male	26/07/1930	-116.5484	45.1878	-21.52	8.69	-84.38	10.47	-14.80	KU Natural History Museum
KU-83753	Iso.	Male	28/07/1960	-109.2302	47.22123	-22.36	9.84	-98.2	9.34	-15.33	KU Natural History Museum
KU-83754	Iso.	Male	28/07/1960	-109.2302	47.22123	-24.07	9.85	-106.73	8.99	-17.04	KU Natural History Museum
MVZ-120300	Iso.	Male	20/08/1955	-120.2399175	39.4319691	-22.97	7.23	-111.39	1.7	-16.01	Museum of Vertebrate Zoology
MVZ-121880	Iso.	Male	23/08/1957	-123.691986	41.5870224	-24.11	7.67	-104.36	3.39	-17.12	Museum of Vertebrate Zoology
MVZ-132569	Iso.	Male	18/07/1952	-122.8441182	39.7275109	-21.89	6.35	-65.33	12.42	-14.96	Museum of Vertebrate Zoology
MVZ-13802	Iso.	Male	04/08/1911	-122.6920885	41.3426373	-21.74	7.21	-77.49	10.55	-15.12	Museum of Vertebrate Zoology
MVZ-3281	Iso.	Male	04/08/1904	-122.178	41.348	-21.85	6.21	-73.555	10.935	-15.25	Museum of Vertebrate Zoology
MVZ-3282	Iso.	Male	04/08/1904	-122.178	41.348	-21.62	6.44	-48.99	11.04	-15.02	Museum of Vertebrate Zoology

MVZ-43802	Iso.	Female	10/08/1929	-122.1667	53.05	-23.59	7.05	-120.96	6.81	-16.87	Museum of Vertebrate Zoology
MVZ-43803	Iso.	Female	12/08/1929	-122.1667	53.05	-23.21	6.92	-120.68	6.99	-16.49	Museum of Vertebrate Zoology
MVZ-43804	Iso.	Male	15/08/1929	-122.1667	53.05	-23.56	6.29	-117.53	7.76	-16.84	Museum of Vertebrate Zoology
MVZ-53772	Iso.	Male	09/07/1927	-122.95	50.1333	-23.11	6.4	-121.32	7.67	-16.41	Museum of Vertebrate Zoology
MVZ-69081	Iso.	Male	17/07/1935	-123.625462	41.9955479	-21.49	7.46	-98.1	8.15	-14.73	Museum of Vertebrate Zoology
MVZ-71455	Iso.	Male	19/07/1930	-122.8435576	39.1232828	NA	6.29	-50.66	11.52	NA	Museum of Vertebrate Zoology
MVZ-87034	Iso.	Male	06/07/1939	-121.5208	45.4189	-21.8	7.48	-73.75	11.41	-15.01	Museum of Vertebrate Zoology
MVZ-94198	Iso.	Male	22/07/1940	-122.9445	45.713	-22.725	7.56	-71.04	9.81	-15.92	Museum of Vertebrate Zoology
MVZ-94199	Iso.	Male	23/07/1940	-122.9445	45.713	-24.07	8.21	-81.015	10.635	-17.27	Museum of Vertebrate Zoology
PSM-14878	Iso.	Male	02/07/1972	-122.2016	44.2289	-23.04	5.51	-69.93	9.46	-15.82	Puget Sound Museum of Natural History
PSM-14879	Iso.	Male	05/07/1972	-122.2116	44.2289	-23.97	6.8	-126.25	6.44	-16.75	Puget Sound Museum of Natural History
PSM-14880	Iso.	Male	01/07/1972	-122.1717	44.2289	-21.92	6.91	-74.77	9.61	-14.70	Puget Sound Museum of Natural History
PSM-14882	Iso.	Male	08/08/1972	-123.922106	45.03337972	-24.76	8.53	-68.41	10.27	-17.54	Puget Sound Museum of Natural History
PSM-1922	Iso.	Male	18/08/1937	-117.0325	45.1642	-22.51	10.86	-115.29	8.24	-15.73	Puget Sound Museum of Natural History
PSM-20460	Iso.	Male	04/08/1974	-118.19167	48.45722	-25.04	8.04	-141.76	17.9	-17.78	Puget Sound Museum of Natural History
PSM-20527	Iso.	Male	22/08/1974	-121.6034	44.3563	-22.43	6.61	-96.15	9.14	-15.17	Puget Sound Museum of Natural History
PSM-20528	Iso.	Male	24/08/1974	-123.3164	44.6365	-22.66	7.7	-60.96	9.55	-15.40	Puget Sound Museum of Natural History
PSM-20531	Iso.	Male	29/08/1974	-123.3479	42.5728	-21.8	5.63	-64.9	11.22	-14.54	Puget Sound Museum of Natural History
PSM-20532	Iso.	Male	29/08/1974	-123.3479	42.5728	-22.99	6.57	-75.51	10.64	-15.73	Puget Sound Museum of Natural History
PSM-20534	Iso.	Male	28/08/1974	-122.5696	42.0334	-22.14	5.3	-65.87	18.39	-14.88	Puget Sound Museum of Natural History
PSM-20552	Iso.	Male	04/08/1975	-118.7593	42.7298	-25.28	8.37	-128.84	6.23	-18.00	Puget Sound Museum of Natural History
PSM-20553	Iso.	Male	12/08/1975	-117.4019	45.7125	-22.11	6.17	-82.59	10.27	-14.83	Puget Sound Museum of Natural History
PSM-20554	Iso.	Male	12/08/1975	-117.4019	45.7125	-22.48	7.15	-85.55	10.52	-15.20	Puget Sound Museum of Natural History
PSM-20555	Iso.	Male	13/08/1975	-117.441	45.7289	-22.19	6.8	-83.91	10.98	-14.91	Puget Sound Museum of Natural History
PSM-21316	Iso.	Male	23/07/1976	-118.5128	45.2242	-22.64	6.69	-81.14	9.53	-15.34	Puget Sound Museum of Natural History
PSM-21318	Iso.	Male	26/07/1976	-117.441	45.7289	-22.13	7	-85.64	10.44	-14.83	Puget Sound Museum of Natural History
PSM-21319	Iso.	Male	26/07/1976	-117.441	45.7289	-22.89	7.67	-95.83	9.4	-15.59	Puget Sound Museum of Natural History
PSM-21322	Iso.	Male	26/07/1976	-117.441	45.7289	-24.49	8.21	-119.68	8.3	-17.19	Puget Sound Museum of Natural History
PSM-21720	Trac.	Male	17/01/1976	-122.20306	47.09806	-24.46	6.33	-78.58	9.6	-17.16	Puget Sound Museum of Natural History
PSM-21721	Trac.	Male	23/01/1976	-122.7556	47.2092	-25.19	8.53	-131.1	6.05	-17.89	Puget Sound Museum of Natural History
PSM-24192	Iso.	Male	20/07/1971	-122.8744	42.2253	-21.85	6.15	-58.18	11.5	-14.65	Puget Sound Museum of Natural History
PSM-25501	Iso.	Male	11/08/1977	-117.4097	45.7436	-22.33	10.1	-103.84	8.65	-15.01	Puget Sound Museum of Natural History
PSM-25508	Iso.	Male	12/08/1977	-117.41971	45.740276	-23.78	9.09	-101.12	8.71	-16.46	Puget Sound Museum of Natural History
PSM-25509	Iso.	Male	12/08/1977	-117.41971	45.740276	-23.54	7.71	-105.31	8.4	-16.22	Puget Sound Museum of Natural History
PSM-25520	Iso.	Female	12/08/1977	-121.0666	44.5204	-21.94	7.42	-82.56	9.7	-14.62	Puget Sound Museum of Natural History
PSM-25521	Iso.	Male	12/08/1977	-121.0666	44.5204	-22.96	7.89	-94.7	9.6	-15.64	Puget Sound Museum of Natural History
PSM-25522	Iso.	Male	11/07/1977	-121.0666	44.5204	-21.93	6.14	-93.07	10.15	-14.61	Puget Sound Museum of Natural History

PSM-25523	Iso.	Male	11/07/1977	-121.0666	44.5204	-21.85	7.27	-80.96	10.72	-14.53	Puget Sound Museum of Natural History
PSM-25524	Iso.	Male	11/07/1977	-121.0666	44.5204	-24.43	6.51	-125.59	6.47	-17.11	Puget Sound Museum of Natural History
PSM-25525	Iso.	Female	11/07/1977	-121.0666	44.5204	-22.94	7.51	-98.39	9.37	-15.62	Puget Sound Museum of Natural History
PSM-25526	Iso.	Male	11/07/1977	-121.0666	44.5204	-22.48	6.19	-72.59	10.98	-15.16	Puget Sound Museum of Natural History
PSM-3756	Iso.	Male	08/08/1952	-116.9447	48.6339	-22.88	6.14	-119.83	7.08	-15.95	Puget Sound Museum of Natural History
PSM-4040	Trac.	Male	22/02/1953	-122.44306	47.25306	-22.08	6.24	-103.36	8.88	-15.14	Puget Sound Museum of Natural History
PSM-6329	Trac.	Female	27/11/1956	-122.532985	47.309393	-26.77	11.07	-125.75	7.13	-19.80	Puget Sound Museum of Natural History
PSM-6804	Iso.	Male	25/08/1956	-117.5329678	46.47167	-23.76	7.01	-130.01	6.55	-16.79	Puget Sound Museum of Natural History
PSM-7694	Trac.	Male	09/10/1946	-122.6762071	45.5234515	-22.58	4.57	-114.34	9.16	-15.72	Puget Sound Museum of Natural History
PSM-7696	Iso.	Male	29/08/1950	-123.4583	42.0225	-21.44	7.28	-86.56	10.25	-14.54	Puget Sound Museum of Natural History
RBCM-10797	Iso.	Male	07/08/1981	-127.7691776	50.11371754	-25.39	7.19	-129.34	8.51	-17.99	Royal British Columbia Museum
RBCM-10798	Iso.	Male	17/08/1981	-127.7691776	50.11371754	-25.02	9.21	-114.69	9.57	-17.62	Royal British Columbia Museum
RBCM-1134	Iso.	Male	07/07/1925	-123.4869013	48.45510717	-23.26	6.61	-97.83	8.28	-16.57	Royal British Columbia Museum
RBCM-15315	Iso.	Male	20/08/1985	-120.3114056	50.66476093	-23.795	10.535	-134.715	6.8	-16.30	Royal British Columbia Museum
RBCM-15355	Trac.	Female	17/12/1985	-123.3514679	48.42861097	-25.41	7.94	-135.12	8.3	-17.91	Royal British Columbia Museum
RBCM-19432	Iso.	Male	27/07/1994	-123.596615	48.361359	-24.005	6.99	-112.51	8.375	-16.26	Royal British Columbia Museum
RBCM-4525	Iso.	Male	11/08/1939	-128.7322464	52.92535054	-23.585	7.01	-120.93	8.83	-16.79	Royal British Columbia Museum
RBCM-4772	Iso.	Male	05/08/1941	-121.4293539	49.38101881	-22.405	7.485	-107.335	9.175	-15.59	Royal British Columbia Museum
RBCM-5163	Iso.	Male	11/08/1945	-120.7822014	49.06452342	-22.86	6.21	-96.67	9.66	-16.01	Royal British Columbia Museum
RBCM-5164	Iso.	Male	12/08/1945	-120.7822014	49.06452342	-22.055	5.39	-105.11	9.825	-15.21	Royal British Columbia Museum
RBCM-5193	Iso.	Male	14/08/1945	-120.6321254	49.11101554	-22.46	6.38	-92.36	10.45	-15.61	Royal British Columbia Museum
RBCM-5194	Iso.	Male	14/08/1945	-120.6321254	49.11101554	-22.44	6.54	-102.41	10.53	-15.59	Royal British Columbia Museum
RBCM-5498	Iso.	Male	15/07/1949	-121.1708	49.2433	-23.43	6.89	-103.34	9.15	-16.54	Royal British Columbia Museum
RBCM-7336	Trac.	Male	17/11/1969	-123.3514679	48.42861097	-23.36	6.82	-116	9.32	-16.19	Royal British Columbia Museum
RBCM-9758	Iso.	Male	06/07/1976	-118.3813556	49.50937246	-23.57	5.71	-109.35	9.25	-16.27	Royal British Columbia Museum
ROM-19783	Iso.	Female	25/07/1949	-114.02902	47.87555	NA	NA	-99	NA	NA	Fraser et al. 2017
ROM-19784	Iso.	Female	25/07/1949	-114.02902	47.87555	NA	NA	-100	NA	NA	Fraser et al. 2017
ROM-22946	Iso.	Female	14/08/1939	-106.5	51.8166667	NA	NA	-91	NA	NA	Fraser et al. 2017
ROM-29539	Iso.	Male	31/08/1941	-119.3666667	50.2	NA	NA	-102	NA	NA	Fraser et al. 2017
ROM-3012190006	Excl.	Female	22/08/1930	-117.2666667	52.9166667	-25.3	8.47	-128.745	5.62	-18.58	Royal Ontario Museum
UBCBBM-M000755	Trac.	Male	03/10/1965	-122.961604	49.247137	-24.49	8.89	-124.74	7.73	-17.39	Beaty Biodiversity Museum
UBCBBM-M002046	Iso.	Male	02/08/1946	-132.087597	53.255818	-23.235	7.575	-70.19	8.595	-16.38	Beaty Biodiversity Museum
UBCBBM-M002047	Iso.	Male	03/08/1946	-132.087597	53.255818	-21.66	8.86	-60.01	8.21	-14.80	Beaty Biodiversity Museum
UBCBBM-M005394	Iso.	Female	04/08/1931	-124.045	52.338611	-18.87	6.5	-142.08	6.81	-12.14	Beaty Biodiversity Museum
UBCBBM-M005395	Iso.	Female	04/08/1931	-124.045	52.338611	-21.27	7.29	-133.79	6.75	-14.54	Beaty Biodiversity Museum
UBCBBM-M005397	Iso.	Female	09/08/1931	-124.045	52.338611	-20.1	7.28	-134.41	6.57	-13.37	Beaty Biodiversity Museum
UBCBBM-M005401	Iso.	Female	28/08/1950	-124.266279	48.873687	-23.35	7.45	-118.25	7.93	-16.45	Beaty Biodiversity Museum

UBCBBM-M005402	Iso.	Female	10/07/1931	-119.336111	49.038611	-23.07	7.58	-96.9	9.96	-16.34	Beaty Biodiversity Museum
UBCBBM-M005403	Iso.	Female	10/07/1931	-119.336111	49.038611	-21.58	7.11	-87.69	10.96	-14.85	Beaty Biodiversity Museum
UBCBBM-M005404	Iso.	Male	07/08/1924	-120.786304	50.111415	-22.98	7.29	-100.06	8.73	-16.30	Beaty Biodiversity Museum
UBCBBM-M010755	Trac.	Male	17/01/1972	-123.240857	49.355816	-25.11	7.04	-109.28	7.97	-17.89	Beaty Biodiversity Museum
UBCBBM-M017232	Trac.	Female	21/12/1931	-123.199824	49.264199	-23.58	7.74	-114.94	8.38	-16.85	Beaty Biodiversity Museum
UBCBBM-M017233	Trac.	Female	01/03/1929	-123.199824	49.264199	-23.76	7.62	-121.95	7.04	-17.04	Beaty Biodiversity Museum
UBCBBM-WRA-05-2377	Trac.	Male	25/10/2005	-122.961604	49.247137	-25.38	7.84	-125.36	6.32	-17.26	Beaty Biodiversity Museum
UBCBBM-WRA-07-2268	Trac.	Male	21/10/2007	-123.131882	49.155742	-25.96	7.42	-130.72	5.31	-17.76	Beaty Biodiversity Museum
UBCBBM-WRA-07-2362	Trac.	Male	09/11/2007	-122.806701	49.026997	-23.89	9.97	-114.17	6.59	-15.69	Beaty Biodiversity Museum
UBCBBM-WRA-10-0150	Trac.	Male	23/02/2012	-123.066609	49.317969	-25.07	7.28	-135.85	6.81	-16.66	Beaty Biodiversity Museum
UBCBBM-WRA-14-3412	Iso.	Male	25/08/2014	-123.108805	49.247791	-26.36	7.59	-112.31	7.39	-17.86	Beaty Biodiversity Museum
UBCBBM-WRA-14-4415	Trac.	Female	03/12/2014	-122.609022	49.228812	-27.63	10.31	-126.38	3.87	-19.13	Beaty Biodiversity Museum
UBCBBM-WRA-14-4538	Trac.	Female	31/12/2014	-122.609022	49.228812	-25.45	7.09	-123.87	4.95	-16.95	Beaty Biodiversity Museum
UBCBBM-WRA-15-0050	Trac.	Female	10/01/2015	-122.951721	49.324543	-24.97	6.17	-118.43	6.67	-16.42	Beaty Biodiversity Museum
UBCBBM-WRA-15-0258	Trac.	Female	18/02/2015	-123.108805	49.247791	-26.43	8.24	-125.22	5.36	-17.88	Beaty Biodiversity Museum
UBCBBM-WRA-15-5023	Trac.	Female	14/10/2015	-122.801701	49.069979	-25.16	10.1	-116.69	4.7	-16.61	Beaty Biodiversity Museum
UBCBBM-WRA-19-0137	Trac.	Female	02/02/2019	-122.313486	49.140903	-24.8	8.06	-112.74	5.79	-16.04	Beaty Biodiversity Museum
UMNH-20412	Iso.	Male	18/07/1963	-109.79908	40.90924	-22.19	9.75	-85.15	9.69	-15.12	Natural History Museum of Utah
UMNH-7532	Iso.	Male	10/07/1950	-111.45007	41.36795	-21.63	9.44	-83.76	9.45	-14.73	Natural History Museum of Utah
UMNH-7534	Iso.	Male	10/07/1950	-111.45007	41.36795	-21.59	8.81	-84.25	9.24	-14.69	Natural History Museum of Utah
UMZM-12972	Iso.	Male	11/08/1967	-114.029886	47.875805	-21.39	7.02	-97.43	9.96	-14.26	Philip L. Wright Zoological Museum
UMZM-20380	Iso.	Male	25/08/1980	-108.428818	45.005641	-25.53	8.8	-115.81	6.7	-18.15	Philip L. Wright Zoological Museum
USNM-204428	Iso.	Male	22/07/1914	-121.5539479	44.29077699	NA	NA	-65	NA	NA	Fraser et al. 2017
USNM-204429	Iso.	Male	23/07/1914	-121.5539479	44.29077699	NA	NA	-73	NA	NA	Fraser et al. 2017
USNM-80765	Iso.	Female	25/08/1896	-121.9978775	43.16356808	NA	NA	-97	NA	NA	Fraser et al. 2017
UVIC-2019001	Trac.	Male	14/10/2019	-122.651614	49.167291	-25.12	6.24	-119.84	7.36	-16.36	B.C. Community Bat Program
UVIC-2019002	Trac.	Male	25/09/2019	-123.092691	48.772543	-26.13	7.41	-127.16	6.15	-17.37	K. Nelson Mist Net Survey
UWBM-13-5596	Trac.	Male	08/11/2013	-122.3084262	47.60785112	-24.52	7.71	-107.3	8.5	-16.06	Burke Museum
UWBM-14-5633	Trac.	Male	03/01/2014	-123.1109075	47.21507798	-26.35	7.46	-121.91	7.06	-17.85	Burke Museum
UWBM-14-5663	Trac.	Male	24/02/2014	-122.4788338	47.42564385	-24.8	7.11	-124.52	5.53	-16.30	Burke Museum
UWBM-14-5665	Trac.	Male	26/02/2014	-122.9082423	46.2728341	-25.04	8.84	-104.51	7.11	-16.54	Burke Museum
UWBM-14-5885	Iso.	Male	19/08/2014	-122.0371655	47.61452748	-24.28	5.75	-110.87	7.29	-15.78	Burke Museum
UWBM-17-0363	Iso.	Male	30/06/2017	-117.4233329	47.68347315	-26.04	10.81	-105.71	6.67	-17.39	Burke Museum
UWBM-17-0373	Iso.	Male	28/06/2017	-122.776	46.168	-24.33	5.76	-126.17	5.07	-15.68	Burke Museum
UWBM-17-0393	Iso.	Male	30/08/2017	-121.833	48.02898	-25.78	13.23	-64.08	9.03	-17.13	Burke Museum
UWBM-17-0584	Trac.	Male	02/10/2017	-121.9246708	47.53088163	-26.36	7.52	-138.76	5.59	-17.71	Burke Museum
UWBM-17-0648	Trac.	Female	12/12/2017	-121.9881471	48.03547806	-27.23	9.08	-123.08	6.44	-18.58	Burke Museum

UWBM-18-0083	Trac.	Male	07/01/2018	-123.0509508	48.5330376	-25.67	8.92	-114.35	7.93	-16.97	Burke Museum
UWBM-18-0121	Trac.	Male	11/01/2018	-122.5377891	45.75758714	-23.64	7.15	-81.27	10.1	-14.94	Burke Museum
UWBM-18-0693	Iso.	Male	27/06/2018	-122.1299	47.064861	-23.89	7.57	-115.51	6.87	-15.19	Burke Museum
UWBM-18-0696	Iso.	Male	27/06/2018	-122.455	46.6166	-26.38	8.48	-122.17	5.94	-17.68	Burke Museum
UWBM-18-0773	Iso.	Male	18/07/2018	-120.675	47.9445	-23.51	10.8	-136.09	5.06	-14.81	Burke Museum
UWBM-67020	Iso.	Male	17/08/1994	-122.5244	47.7472	-25.02	5.96	-113.36	7.62	-17.28	Burke Museum
UWBM-67028	Iso.	Male	26/08/1994	-122.7458	48.9939	-26.64	6.58	-145.53	5.45	-18.90	Burke Museum
UWBM-75806	Iso.	Male	20/08/1997	-122.377237	47.766913	-25.57	6.59	-111.58	7.33	-17.73	Burke Museum
UWBM-75811	Trac.	Female	01/11/1998	-122.128884	47.738554	-26.04	7.25	-134.42	3.77	-18.17	Burke Museum
UWBM-79052	Trac.	Male	24/09/1996	-122.6822	47.9256	-26.75	7.09	-129.59	7.16	-18.95	Burke Museum
UWBM-79135	Trac.	Male	13/01/1996	-123.095	46.8219	-24.74	9.97	-117.3	7.25	-16.94	Burke Museum
UWBM-WDFW-170	Trac.	Female	16/02/2018	-122.876558	46.97889	-24.46	7.24	-121.02	4.37	-15.76	Burke Museum
UWBM-WDFW-184	Iso.	Male	22/06/2017	-120.9319	47.175	-23.65	5.74	-99.09	9.18	-15.00	Burke Museum
UWBM-WDFW-193	Trac.	Male	04/12/2019	-122.300014	47.113345	-22.56	5.19	-101.55	8.74	-13.80	Burke Museum

Table A.1: All stable isotope compositions are reported in ‰ and are relative to VPDB, VSMOW, AIR, and VSMOW for carbon, hydrogen, nitrogen, and oxygen respectively. Sample uses included known origin samples used for isoscape development (Iso.), unknown origin samples used for origin tracing (Trac.), and samples excluded from use due to being outside the likely resident period (Excl.)

Appendix B

Model Summaries

Hydrogen

Family: Gaussian

Link function: Identity

Formula:

δ^2H ~ Mean Annual Irradiance + s(Distance from Coast, k = 5, bs = "cr") +

Elevation

Parametric coefficients:

	Estimate	Std. Error	t value	Pr(> $\|t\|$)	
(Intercept)	-1.877e+02	1.352e+01	-13.885	<2e-16	***
Mean Annual Irradiance	7.541e+00	1.168e+00	6.456	1.75e-09	***
Elevation	-1.433e-02	4.801e-03	-2.984	0.00337	**

Approximate significance of smooth terms:

	edf	Ref.df	F	p-value
s(Distance from Coast)	3.697	3.916	2.207	0.139

- - -

Signif. codes: 0 '***' 0.001 '**' 0.01 '*' 0.05 '.' 0.1 ' ' 1

R-sq.(adj) = 0.294 Deviance explained = 32.2%

GCV = 286.92 Scale est. = 273.48 n = 143

Carbon

Family: Gaussian

Link function: Identity

Formula:

$\delta^{13}C_a \sim$ s(Distance from Coast, k = 6, bs = "cr") + s(Mean May to July Irradiance, k = 6, bs = "cr") + s(Mean Annual Relative Humidity)

Parametric coefficients:

	Estimate	Std. Error	t value	Pr($>\|t\|$)	
(Intercept)	-15.7219	0.0756	-208	<2e-16	***

Approximate significance of smooth terms:

	edf	Ref.df	F	p-value	
s(Distance from Coast)	4.567	4.836	4.675	0.00126	**
s(Mean May to July Irradiance)	2.799	2.957	2.267	0.07395	.
s(Mean Annual Relative Humidity)	1.475	1.813	2.100	0.07945	.

- - -

Signif. codes: 0 '***' 0.001 '**' 0.01 '*' 0.05 '.' 0.1 ' ' 1

R-sq.(adj) = 0.294 Deviance explained = 34.2%

GCV = 0.81518 Scale est. = 0.75441 n = 132

Nitrogen

Family: Gaussian

Link function: Identity

Formula:

δ^{15}N ~ s(Distance from Coast, k = 4, bs = "cr") + s(Mean Annual Precipitation, k = 4, bs = "cr") + s(Elevation, k = 4, bs = "cr")

Parametric coefficients:

	Estimate	Std. Error	t value	Pr(> $\|t\|$)	
(Intercept)	8.06063	0.07888	102.2	<2e-16	***

Approximate significance of smooth terms:

	edf	Ref.df	F	p-value	
s(Distance from Coast)	2.037	2.194	34.621	<2e-16	***
s(Mean Annual Precipitation)	2.974	2.999	8.052	6.53e-05	***
s(Elevation)	2.819	2.965	3.848	0.0166	*

- - -

Signif. codes: 0 '***' 0.001 '**' 0.01 '*' 0.05 '.' 0.1 ' ' 1

R-sq.(adj) = 0.615 Deviance explained = 63.8%

GCV = 0.90501 Scale est. = 0.84625 n = 136

References

Adams, H. and McGuire, L. P. (2022). Island biogeography theory and the urban landscape: stopover site selection by the silver-haired bat (*Lasionycteris noctivagans). Canadian Journal of Zoology*, 100(4):243–250.

Alves, J. A., Gunnarsson, T. G., Hayhow, D. B., Appleton, G. F., Potts, P. M., Sutherland, W. J., and Gill, J. A. (2013). Costs, benefits, and fitness consequences of different migratory strategies. *Ecology*, 94(1):11–17.

Amundson, R., Austin, A. T., Schuur, E. a. G., Yoo, K., Matzek, V., Kendall, C., Uebersax, A., Brenner, D., and Baisden, W. T. (2003). Global patterns of the isotopic composition of soil and plant nitrogen. *Global Biogeochemical Cycles*, 17(1).

Areta, J. and Bodrati, A. (2008). Seasonal movements and phylogenetic affinity of the shear-tailed gray-tyrant (*Muscipipra vetula). Ornitologia Neotropical*, 19:201–211.

Arnett, E. B. and Baerwald, E. F. (2013). Impacts of wind energy development on bats: Implications for conservation. In Adams, R. A. and Pedersen, S. C., editors, *Bat Evolution, Ecology, and Conservation*, pages 435–456. Springer, New York, NY.

Arnett, E. B., Baerwald, E. F., Mathews, F., Rodrigues, L., Rodríguez-Durán, A.,

Rydell, J., Villegas-Patraca, R., and Voigt, C. C. (2016). Impacts of wind energy development on bats: A global perspective. In Voigt, C. C. and Kingston, T., editors, *Bats in the Anthropocene: Conservation of Bats in a Changing World*, pages 295–323. Springer International Publishing, Cham.

Arnett, E. B., Brown, W. K., Erickson, W. P., Fiedler, J. K., Hamilton, B. L., Henry, T. H., Jain, A., Johnson, G. D., Kerns, J., Koford, R. R., Nicholson, C. P., O'Connell, T. J., Piorkowski, M. D., and Tankersley, R. D. (2008). Patterns of bat fatalities at wind energy facilities in North America. *The Journal of Wildlife Management*, 72(1):61–78.

Arnett, E. B., Hein, C. D., Schirmacher, M. R., Huso, M. M. P., and Szewczak, J. M. (2013). Evaluating the effectiveness of an ultrasonic acoustic deterrent for reducing bat fatalities at wind turbines. *PLoS ONE*, 8(6):e65794.

Arnett, E. B., Huso, M. M., Schirmacher, M. R., and Hayes, J. P. (2011). Altering turbine speed reduces bat mortality at wind-energy facilities. *Frontiers in Ecology and the Environment*, 9(4):209–214.

Baerwald, E. F. and Barclay, R. M. R. (2009). Geographic variation in activity and fatality of migratory bats at wind energy facilities. *Journal of Mammalogy*, 90(6):1341–1349.

Baerwald, E. F., Edworthy, J., Holder, M., and Barclay, R. M. R. (2009). A large-scale mitigation experiment to reduce bat fatalities at wind energy facilities. *The Journal of Wildlife Management*, 73(7):1077–1081.

Baerwald, E. F., Patterson, W. P., and Barclay, R. M. R. (2014). Origins and migratory patterns of bats killed by wind turbines in southern Alberta: evidence from stable isotopes. *Ecosphere*, 5(9):art118.

Bataille, C. P. and Bowen, G. J. (2012). Mapping 87Sr/86Sr variations in bedrock and water for large scale provenance studies. *Chemical Geology*, 304-305:39–52.

Bataille, C. P., Crowley, B. E., Wooller, M. J., and Bowen, G. J. (2020). Advances in global bioavailable strontium isoscapes. *Palaeogeography, Palaeoclimatology, Palaeoecology*, 555:109849.

Bataille, C. P., Jaouen, K., Milano, S., Trost, M., Steinbrenner, S., Crubézy, É., and Colleter, R. (2021). Triple sulfur-oxygen-strontium isotopes probabilistic geographic assignment of archaeological remains using a novel sulfur isoscape of western Europe. *PLoS ONE*, 16(5).

Bauer, S., McNamara, J. M., and Barta, Z. (2020). Environmental variability, reliability of information and the timing of migration. *Proceedings of the Royal Society B: Biological Sciences*, 287(1926):20200622.

BCStats (2022). 2021 Sub-Provincial Population Estimates Highlights. Technical report.

Beilke, E. A. and O'Keefe, J. M. (2023). Bats reduce insect density and defoliation in temperate forests: An exclusion experiment. *Ecology*, 104(2):e3903.

Bernard, R. F., Foster, J. T., Willcox, E. V., Parise, K. L., and McCracken, G. F. (2015). Molecular detection of the causative agent of white-nose syndrome on Rafinesque's big-eared bats (*Corynorhinus rafinesquii*) and two species of migratory bats in the southeastern USA. *Journal of Wildlife Diseases*, 51(2):519–522.

Blehert, D. S., Hicks, A. C., Behr, M., Meteyer, C. U., Berlowski-Zier, B. M., Buckles, E. L., Coleman, J. T. H., Darling, S. R., Gargas, A., Niver, R., Okoniewski, J. C., Rudd, R. J., and Stone, W. B. (2009). Bat White-Nose Syndrome: An Emerging Fungal Pathogen? *Science*, 323(5911):227–227.

Bowen, G. J. (2010). Isoscapes: Spatial Pattern in Isotopic Biogeochemistry. *Annual Review of Earth and Planetary Sciences*, 38(1):161–187.

Bowen, G. J., Wassenaar, L. I., and Hobson, K. A. (2005). Global Application of Stable Hydrogen and Oxygen Isotopes to Wildlife Forensics. *Oecologia*, 143(3):337–348.

Bowling, D. R., McDowell, N. G., Bond, B. J., Law, B. E., and Ehleringer, J. R. (2002). 13C Content of Ecosystem Respiration Is Linked to Precipitation and Vapor Pressure Deficit. *Oecologia*, 131(1):113–124.

Boyles, J. G., Cryan, P. M., McCracken, G. F., and Kunz, T. H. (2011). Economic Importance of Bats in Agriculture. *Science*, 332(6025):41–42.

Brewer, C. T., Rauch-Davis, W. A., and Fraser, E. E. (2021). The Use of Intrinsic Markers for Studying the Migratory Movements of Bats. *Animals : an Open Access Journal from MDPI*, 11(12).

Britzke, E. R., Loeb, S. C., Hobson, K. A., Romanek, C. S., and Vonhof, M. J. (2009). Using hydrogen isotopes to assign origins of bats in the eastern United States. *Journal of Mammalogy*, 90(3):743–751.

Broennimann, O., Fitzpatrick, M. C., Pearman, P. B., Petitpierre, B., Pellissier, L., Yoccoz, N. G., Thuiller, W., Fortin, M.-J., Randin, C., Zimmermann, N. E., Graham, C. H., and Guisan, A. (2012). Measuring ecological niche overlap from occurrence and spatial environmental data. *Global Ecology and Biogeography*, 21(4):481–497.

Brown, J. M., Bouten, W., Camphuysen, K. C. J., Nolet, B. A., and Shamoun-Baranes, J. (2023). Energetic and behavioral consequences of migration: an

empirical evaluation in the context of the full annual cycle. *Scientific Reports*, 13(1):1–15.

Buechley, E. R., Oppel, S., Efrat, R., Phipps, W. L., Carbonell Alanís, I., Álvarez, E., Andreotti, A., Arkumarev, V., Berger-Tal, O., Bermejo Bermejo, A., Bounas, A., Ceccolini, G., Cenerini, A., Dobrev, V., Duriez, O., García, J., García-Ripollés, C., Galán, M., Gil, A., Giraud, L., Hatzofe, O., Iglesias-Lebrija, J. J., Karyakin, I., Kobierzycki, E., Kret, E., Loercher, F., López-López, P., Miller, Y., Mueller, T., Nikolov, S. C., de la Puente, J., Sapir, N., Saravia, V., Şekercioğlu, Ç. H., Sillett, T. S., Tavares, J., Urios, V., and Marra, P. P. (2021). Differential survival throughout the full annual cycle of a migratory bird presents a life-history trade-off. *Journal of Animal Ecology*, 90(5):1228–1238.

Campbell, C. J., Fitzpatrick, M. C., Zanden, H. B. V., and Nelson, D. M. (2020). Advancing interpretation of stable isotope assignment maps: comparing and summarizing origins of known-provenance migratory bats. *Animal Migration*, 7(1):27–41.

Campbell, C. J., Nelson, D. M., Gates, J. E., Gibbs, H. L., Stevenson, E. R., Johnson, B., Nagel, J., Trott, R., Wieringa, J. G., and Zanden, H. B. V. (2022). White-nose syndrome pathogen *Pseudogymnoascus destructans* detected in migratory tree-roosting bats. *Journal of Wildlife Diseases*, 58(3):652–657.

Cardoso, P., Barton, P. S., Birkhofer, K., Chichorro, F., Deacon, C., Fartmann, T., Fukushima, C. S., Gaigher, R., Habel, J. C., Hallmann, C. A., Hill, M. J., Hochkirch, A., Kwak, M. L., Mammola, S., Ari Noriega, J., Orfinger, A. B., Pedraza, F., Pryke, J. S., Roque, F. O., Settele, J., Simaika, J. P., Stork, N. E., Suhling, F., Vorster, C., and Samways, M. J. (2020). Scientists' warning to humanity on insect extinctions. *Biological Conservation*, 242:108426.

Casey, M. M. and Post, D. M. (2011). The problem of isotopic baseline: Reconstructing the diet and trophic position of fossil animals. *Earth-Science Reviews*, 106(1-2):131–148.

Cheng, T. L., Mayberry, H., McGuire, L. P., Hoyt, J. R., Langwig, K. E., Nguyen, H., Parise, K. L., Foster, J. T., Willis, C. K. R., Kilpatrick, A. M., and Frick, W. F. (2017). Efficacy of a probiotic bacterium to treat bats affected by the disease white-nose syndrome. *Journal of Applied Ecology*, 54(3):701–708.

Chételat, J., Hickey, M. B. C., Poulain, A. J., Dastoor, A., Ryjkov, A., McAlpine, D., Vanderwolf, K., Jung, T. S., Hale, L., Cooke, E. L., Hobson, D., Jonasson, K., Kaupas, L., McCarthy, S., McClelland, C., Morningstar, D., Norquay, K. J., Novy, R., Player, D., Redford, T., Simard, A., Stamler, S., Webber, Q. M., Yumvihoze, E., and Zanuttig, M. (2018). Spatial variation of mercury bioaccumulation in bats of Canada linked to atmospheric mercury deposition. *Science of The Total Environment*, 626:668–677.

COSEWIC (2023). COSEWIC assessment and status report on the hoary bat (*Lasiurus cinereus*), eastern red bat (*Lasiurus borealis*), silver-haired bat (*Lasionycteris noctivagans*). Technical report, Committee on the Status of Endangered Wildlife in Canada, Gatineau, QC, Canada.

Cryan, P. M. (2003). Seasonal distribution of migratory tree bats (*Lasiurus* and *Lasionycteris*) in North America. *Journal of Mammalogy*, 84(2):579–593.

Cryan, P. M., Bogan, M. A., Rye, R. O., Landis, G. P., and Kester, C. L. (2004). Stable hydrogen isotope analysis of bat hair as evidence for seasonal molt and long-distance migration. *Journal of Mammalogy*, 85(5):995–1001.

Cryan, P. M., Stricker, C. A., and Wunder, M. B. (2012). Evidence of cryptic individ-

ual specialization in an opportunistic insectivorous bat. *Journal of Mammalogy*, 93(2):381–389.

Cryan, P. M., Stricker, C. A., and Wunder, M. B. (2014). Continental-scale, seasonal movements of a heterothermic migratory tree bat. *Ecological Applications*, 24(4):602–616.

Danielson, J. and Gesch, D. (2011). Global multi-resolution terrain elevation data 2010 (GMTED2010).

Dansgaard, W. (1964). Stable isotopes in precipitation. *Tellus*, 16(4):436–468.

Davenport, L. C., Bazán, I. N., and Erazo, N. C. (2012). East with the night: Longitudinal migration of the Orinoco goose (*Neochen jubata*) between Manú National Park, Peru and the Llanos de Moxos, Bolivia. *PLOS ONE*, 7(10):e46886.

Dingle, H. and Drake, V. A. (2007). What is migration? *BioScience*, 57(2):113–121.

Dufour, P., de Franceschi, C., Doniol-Valcroze, P., Jiguet, F., Guéguen, M., Renaud, J., Lavergne, S., and Crochet, P.-A. (2021). A new westward migration route in an Asian passerine bird. *Current Biology*, 31(24):5590–5596.e4.

Dzal, Y., Hooton, L. A., Clare, E. L., and Fenton, M. B. (2009). Bat Activity and Genetic Diversity at Long Point, Ontario, an Important Bird Stopover Site. *Acta Chiropterologica*, 11(2):307–315.

Ellison, L. (2008). Summary and analysis of the US government bat banding program. Open-File Report, U.S. Geological Survey, Fort Collins, CO, USA.

Environment Canada (2015). Little brown myotis (*Myotis lucifugus*), northern myotis (*Myotis septentrionalis*), and tri-colored bat (*Perimyotis subflavus).* Technical report, Environment Canada, Ottawa, ON, Canada.

ESRI (2020). ArcGIS Desktop: Release 10.8.1.

Falxa, G. (2007). Winter Foraging of Silver-Haired and California Myotis Bats in Western Washington. *Northwestern Naturalist*, 88(2):98–100.

Fleming, T. and Eby, P. (2003). Ecology of bat migration. In Kunz, T. and Fenton, M., editors, *Bat Ecology*, pages 156–208. The University of Chicago Press, Chicago, Illinois, USA.

Fletcher, Q. E., Webber, Q. M. R., and Willis, C. K. R. (2020). Modelling the potential efficacy of treatments for white-nose syndrome in bats. *Journal of Applied Ecology*, 57(7):1283–1291.

Foley, J., Clifford, D., Castle, K., Cryan, P., and Ostfeld, R. S. (2011). Investigating and Managing the Rapid Emergence of White-Nose Syndrome, a Novel, Fatal, Infectious Disease of Hibernating Bats. *Conservation Biology*, 25(2):223–231.

Francey, R. J., Allison, C. E., Etheridge, D. M., Trudinger, C. M., Enting, I. G., Leuenberger, M., Langenfelds, R. L., Michel, E., and Steele, L. P. (1999). A 1000-year high precision record of δ13C in atmospheric CO2. *Tellus B: Chemical and Physical Meteorology*, 51(2):170–193.

Fraser, E., Longstaffe, F., and Fenton, M. (2013). Moulting matters: the importance of understanding moulting cycles in bats when using fur for endogenous marker analysis. *Canadian Journal of Zoology*, 91(8):533–544.

Fraser, E. E. (2011). *Stable isotope analyses of bat fur: Applications for investigating North American bat migration.* PhD thesis, The University of Western Ontario, London, Ontario, Canada.

Fraser, E. E., Brooks, D., and Longstaffe, F. J. (2017). Stable isotope investigation of the migratory behavior of silver-haired bats (*Lasionycteris noctivagans*) in eastern North America. *Journal of Mammalogy*, 98(5):1225–1235.

Fraser, E. E., McGuire, L. P., Eger, J. L., Longstaffe, F. J., and Fenton, M. B. (2012). Evidence of latitudinal migration in tri-colored bats, *Perimyotis subflavus*. *PLoS ONE*, 7(2):e31419.

Fraser, E. E., Miller, J. F., Longstaffe, F. J., and Fenton, M. B. (2015). Systematic variation in the stable hydrogen isotope (δ2H) composition of fur from summer populations of two species of temperate insectivorous bats. *Mammalian Biology*, 80(4):278–284.

Frick, W. F., Baerwald, E. F., Pollock, J. F., Barclay, R. M. R., Szymanski, J. A., Weller, T. J., Russell, A. L., Loeb, S. C., Medellin, R. A., and McGuire, L. P. (2017). Fatalities at wind turbines may threaten population viability of a migratory bat. *Biological Conservation*, 209:172–177.

Frick, W. F., Kingston, T., and Flanders, J. (2020). A review of the major threats and challenges to global bat conservation. *Annals of the New York Academy of Sciences*, 1469(1):5–25.

Frick, W. F., Pollock, J. F., Hicks, A. C., Langwig, K. E., Reynolds, D. S., Turner, G. G., Butchkoski, C. M., and Kunz, T. H. (2010). An Emerging Disease Causes Regional Population Collapse of a Common North American Bat Species. *Science*, 329(5992):679–682.

Furey, N. M. and Racey, P. A. (2016). Conservation Ecology of Cave Bats. In Voigt, C. C. and Kingston, T., editors, *Bats in the Anthropocene: Conservation of Bats in a Changing World*, pages 463–500. Springer International Publishing, Cham.

Furmankiewicz, J. and Kucharska, M. (2009). Migration of Bats along a Large River Valley in Southwestern Poland. *Journal of Mammalogy*, 90(6):1310–1317.

Gonsalves, L., Law, B., Webb, C., and Monamy, V. (2013). Foraging Ranges of Insectivorous Bats Shift Relative to Changes in Mosquito Abundance. *PLOS ONE*, 8(5):e64081.

Grider, J., Thogmartin, W. E., Grant, E. H. C., Bernard, R. F., and Russell, R. E. (2022). Early treatment of white-nose syndrome is necessary to stop population decline. *Journal of Applied Ecology*, 59(10):2531–2541.

Haest, B., Stepanian, P. M., Wainwright, C. E., Liechti, F., and Bauer, S. (2021). Climatic drivers of (changes in) bat migration phenology at Bracken Cave (USA). *Global Change Biology*, 27(4):768–780.

Hayes, M. A. (2013). Bats Killed in Large Numbers at United States Wind Energy Facilities. *BioScience*, 63(12):975–979.

Hayes, M. A., Hooton, L. A., Gilland, K. L., Grandgent, C., Smith, R. L., Lindsay, S. R., Collins, J. D., Schumacher, S. M., Rabie, P. A., Gruver, J. C., and Goodrich-Mahoney, J. (2019). A smart curtailment approach for reducing bat fatalities and curtailment time at wind energy facilities. *Ecological Applications*, 29(4):e01881.

Hedenström, A. (2009). Optimal Migration Strategies in Bats. *Journal of Mammalogy*, 90(6):1298–1309.

Hijmans, R. J. (2023). *terra: Spatial Data Analysis*. R package version 1.7-65.

Hobson, K. A. (1999). Tracing origins and migration of wildlife using stable isotopes: a review. *Oecologia*, 120(3):314–326.

Hobson, K. A. and Wassenaar, L. I., editors (2008). *Tracking animal migration with stable isotopes*. Number v. 2 in Terrestrial ecology series. Academic Press, Amsterdam ; Boston, 1st ed edition.

Hobson, K. A., Wassenaar, L. I., and Taylor, O. R. (1999). Stable Isotopes (δD and δ 13C) Are Geographic Indicators of Natal Origins of Monarch Butterflies in Eastern North America. *Oecologia*, 120(3):397–404.

Hoefs, J. (2018). *Stable Isotope Geochemistry*. Springer Textbooks in Earth Sciences, Geography and Environment. Springer International Publishing, Cham.

Holliday, C., Wisby, J. P., Roby, P. L., Samoray, S. T., and Vannatta, J. M. (2023). Modeling migration and movement of gray bats. *The Journal of Wildlife Management*, 87(3):e22364.

Huebschman, J. J., Hoerner, S. A., White, J. P., Kaarakka, H. M., Parise, K. L., and Foster, J. T. (2019). Detection of *Pseudogymnoascus destructans* on Wisconsin bats during summer. *Journal of Wildlife Diseases*, 55(3):673–677.

Izor, R. J. (1979). Winter Range of the Silver-Haired Bat. *Journal of Mammalogy*, 60(3):641–643.

Jameson, J. W. and Willis, C. K. R. (2014). Activity of tree bats at anthropogenic tall structures: implications for mortality of bats at wind turbines. *Animal Behaviour*, 97:145–152.

Jonasson, K. A. and Guglielmo, C. G. (2016). Sex differences in spring migration timing and body composition of silver-haired bats Lasionycteris noctivagans. *Journal of Mammalogy*, 97(6):1535–1542.

Killingley, J. S. (1980). Migrations of California Gray Whales Tracked by Oxygen-18 Variations in their Epizoic Barnacles. *Science*, 207(4432):759–760.

Kunz, T. H., Arnett, E. B., Erickson, W. P., Hoar, A. R., Johnson, G. D., Larkin, R. P., Strickland, M. D., Thresher, R. W., and Tuttle, M. D. (2007). Ecological Impacts of Wind Energy Development on Bats: Questions, Research Needs, and Hypotheses. *Frontiers in Ecology and the Environment*, 5(6):315–324.

Kunz, T. H., Torrez, E. B. d., Bauer, D., Lobova, T., and Fleming, T. H. (2011). Ecosystem services provided by bats. *Annals of the New York Academy of Sciences*, 1223(1):1–38.

Kunz, T. H., Whitaker, J. O., and Wadanoli, M. D. (1995). Dietary energetics of the insectivorous Mexican free-tailed bat (*Tadarida brasiliensis*) during pregnancy and lactation. *Oecologia*, 101(4):407–415.

Kurta, A., Bell, G. P., Nagy, K. A., and Kunz, T. H. (1989). Energetics of pregnancy and lactation in freeranging little brown bats (*Myotis lucifugus*). *Physiological Zoology*, 62(3):804–818.

Law, B., Park, K. J., and Lacki, M. J. (2016). Insectivorous Bats and Silviculture: Balancing Timber Production and Bat Conservation. In Voigt, C. C. and Kingston, T., editors, *Bats in the Anthropocene: Conservation of Bats in a Changing World*, pages 105–150. Springer International Publishing, Cham.

Lees, A. C. (2016). Evidence for longitudinal migration by a "sedentary" Brazilian flycatcher, the Ash-throated Casiornis. *Journal of Field Ornithology*, 87(3):251–259.

Long, E. S., Sweitzer, R. A., Diefenbach, D. R., and Ben-David, M. (2005). Controlling for anthropogenically induced atmospheric variation in stable carbon isotope studies. *Oecologia*, 146(1):148–156.

Lott, C. A., Meehan, T. D., and Heath, J. A. (2003). Estimating the latitudinal origins of migratory birds using hydrogen and sulfur stable isotopes in feathers: influence of marine prey base. *Oecologia*, 134(4):505–510.

Luo, W., Wang, X., Sardans, J., Wang, Z., Dijkstra, F. A., Lü, X.-T., Peñuelas, J., and Han, X. (2018). Higher capability of C3 than C4 plants to use nitrogen inferred from nitrogen stable isotopes along an aridity gradient. *Plant and Soil*, 428(1):93–103.

Ma, C., Vander Zanden, H. B., Wunder, M. B., and Bowen, G. J. (2020). assignR: An r package for isotope-based geographic assignment. *Methods in Ecology and Evolution*, 11(8):996–1001.

Maslo, B., Mau, R. L., Kerwin, K., McDonough, R., McHale, E., and Foster, J. T. (2022). Bats provide a critical ecosystem service by consuming a large diversity of agricultural pest insects. *Agriculture, Ecosystems & Environment*, 324:107722.

McCarroll, D. and Pawellek, F. (2001). Stable carbon isotope ratios of *Pinus sylvestris* from northern Finland and the potential for extracting a climate signal from long Fennoscandian chronologies. *The Holocene*, 11(5):517–526.

McGuire, L. P., Guglielmo, C. G., Mackenzie, S. A., and Taylor, P. D. (2012). Migratory stopover in the long-distance migrant silver-haired bat, *Lasionycteris noctivagans*. *Journal of Animal Ecology*, 81(2):377–385.

Metcalfe, J. Z. (2021). C3 plant isotopic variability in a boreal mixed woodland: implications for bison and other herbivores. *PeerJ*, 9:e12167.

Micalizzi, E. W., Olson, C. R., Forshner, S. A., and Barclay, R. M. (2023). The flight speed of a migrating silver-haired bat (*Lasionycteris Noctivagans). Northwestern Naturalist*, 104(2):141–144.

Nagorsen, D. W., Bryant, A. A., Kerridge, D., Roberts, G., Roberts, A., and Sarell, M. J. (1993). Winter Bat Records for British Columbia. *Northwestern Naturalist*, 74(3):61–66.

Norquay, K. J. O., Martinez-Nuñez, F., Dubois, J. E., Monson, K. M., and Willis, C. K. R. (2013). Long-distance movements of little brown bats (Myotis lucifugus). *Journal of Mammalogy*, 94(2):506–515.

O'Leary, M. H. (1988). Carbon isotopes in photosynthesis. *Bioscience*, 38(5):328–336.

Palmer, J. M., Drees, K. P., Foster, J. T., and Lindner, D. L. (2018). Extreme sensitivity to ultraviolet light in the fungal pathogen causing white-nose syndrome of bats. *Nature Communications*, 9(1):35.

Peterson, B. J. and Fry, B. (1987). Stable Isotopes in Ecosystem Studies. *Annual Review of Ecology and Systematics*, 18:293–320.

Popa-Lisseanu, A. G., Kramer-Schadt, S., Quetglas, J., Delgado-Huertas, A., Kelm, D. H., and Ibáñez, C. (2015). Seasonal Variation in Stable Carbon and Nitrogen Isotope Values of Bats Reflect Environmental Baselines. *PLOS ONE*, 10(2):e0117052.

Popa-Lisseanu, A. G. and Voigt, C. C. (2009). Bats on the Move. *Journal of Mammalogy*, 90(6):1283–1289.

Puget Sound Regional Council (2022). Puget Sound Trends. Technical report.

Pylant, C. L., Nelson, D. M., and Keller, S. R. (2014). Stable hydrogen isotopes record the summering grounds of eastern red bats (*Lasiurus borealis*). *PeerJ*, 2:e629.

R Core Team (2023). R: A Language and Environment for Statistical Computing.

Reich, M. S., Flockhart, D. T. T., Norris, D. R., Hu, L., and Bataille, C. P. (2021). Continuous-surface geographic assignment of migratory animals using strontium isotopes: A case study with monarch butterflies. *Methods in Ecology and Evolution*, n/a(n/a).

Rocke, T. E., Kingstad-Bakke, B., Wüthrich, M., Stading, B., Abbott, R. C., Isidoro-Ayza, M., Dobson, H. E., dos Santos Dias, L., Galles, K., Lankton, J. S., Falendysz, E. A., Lorch, J. M., Fites, J. S., Lopera-Madrid, J., White, J. P., Klein, B., and Osorio, J. E. (2019). Virally-vectored vaccine candidates against white-nose syndrome induce anti-fungal immune response in little brown bats (*Myotis lucifugus). Scientific Reports*, 9(1):N.PAG–N.PAG.

Schoener, T. W. (1970). Nonsynchronous Spatial Overlap of Lizards in Patchy Habitats. *Ecology*, 51(3):408–418.

Schulze, E.-D., Williams, R. J., Farquhar, G. D., Schulze, W., Langridge, J., Miller, J. M., and Walker, B. H. (1998). Carbon and nitrogen isotope discrimination and nitrogen nutrition of trees along a rainfall gradient in northern Australia. *Functional Plant Biology*, 25(4):413–425.

Segers, J. L. and Broders, H. G. (2015). Carbon (δ13C) and Nitrogen (δ15N) Stable Isotope Signatures in Bat Fur Indicate Swarming Sites Have Catchment Areas for Bats from Different Summering Areas. *PLOS ONE*, 10(4):e0125755.

Smallwood, K. S. (2013). Comparing bird and bat fatality-rate estimates among North American wind-energy projects. *Wildlife Society Bulletin*, 37(1):19–33.

Soto, D. X., Koehler, G., Wassenaar, L. I., and Hobson, K. A. (2017). Re-evaluation of the hydrogen stable isotopic composition of keratin calibration standards for wildlife and forensic science applications: Measurements of H isotopes of keratin

calibration standards. *Rapid Communications in Mass Spectrometry*, 31(14):1193–1203.

Stewart, G. R., Turnbull, M. H., Schmidt, S., and Erskine, P. D. (1995). 13C Natural Abundance in Plant Communities Along a Rainfall Gradient: a Biological Integrator of Water Availability. *Functional Plant Biology*, 22(1):51–55.

Still, C. J., Berry, J. A., Collatz, G. J., and DeFries, R. S. (2003). Global distribution of C $_3$ and C $_4$ vegetation: Carbon cycle implications. *Global Biogeochemical Cycles*, 17(1):6–1–6–14.

Suits, N. S., Denning, A. S., Berry, J. A., Still, C. J., Kaduk, J., Miller, J. B., and Baker, I. T. (2005). Simulation of carbon isotope discrimination of the terrestrial biosphere. *Global Biogeochemical Cycles*, 19(1).

Sullivan, A. R., Bump, J. K., Kruger, L. A., and Peterson, R. O. (2012). Bat-cave catchment areas: using stable isotopes (δD) to determine the probable origins of hibernating bats. *Ecological Applications*, 22(5):1428–1434.

Suzuki, R. and Shimodaira, H. (2006). Pvclust: an R package for assessing the uncertainty in hierarchical clustering. *Bioinformatics*, 22(12):1540–1542.

USFWS (2012). Land-Based Wind Energy Guidelines.

USFWS (2022). Endangered and Threatened Wildlife and Plants; Endangered Species Status for Northern Long-Eared Bat. Technical report, U.S. Fish & Wildlife Service, Washington, DC.

USFWS (2023). White-Nose Syndrome.

USGS (2023). U.S. Wind Turbine Database.

Voigt, C. C., Lehmann, D., and Greif, S. (2015). Stable isotope ratios of hydrogen separate mammals of aquatic and terrestrial food webs. *Methods in Ecology and Evolution*, 6(11):1332–1340.

Vonhof, M. J., Russell, A. L., and Miller-Butterworth, C. M. (2019). Range-wide genetic analysis of little brown bat (*Myotis lucifugus*) populations: Estimating the risk of spread of white-nose syndrome. *PLoS ONE*, 10(7):e0128713.

Wagner, D. L., Grames, E. M., Forister, M. L., Berenbaum, M. R., and Stopak, D. (2021). Insect decline in the Anthropocene: Death by a thousand cuts. *Proceedings of the National Academy of Sciences*, 118(2):e2023989118.

Wang, T., Hamann, A., Spittlehouse, D., and Carroll, C. (2016). Locally downscaled and spatially customizable climate data for historical and future periods for North America. *PLoS ONE*, 11(6).

Wassenaar, L. I. and Hobson, K. A. (2003). Comparative equilibration and online technique for determination of non-exchangeable hydrogen of keratins for use in animal migration studies. *Isotopes in Environmental and Health Studies*, 39(3):211–217.

Weaver, S. P., Hein, C. D., Simpson, T. R., Evans, J. W., and Castro-Arellano, I. (2020). Ultrasonic acoustic deterrents significantly reduce bat fatalities at wind turbines. *Global Ecology and Conservation*, 24:e01099.

Weller, T. J. (2019). *BatAMP: (*Lasionycteris noctivagans) *2006 - 2018*.

Werner, S. J., Fischer, J. W., and Hobson, K. A. (2020). Multi-isotopic (δ2H, δ13C, δ15N) tracing of molt origin for European starlings associated with U.S. dairies and feedlots. *PLoS One; San Francisco*, 15(8):e0237137.

Wieringa, J. G., Carstens, B. C., and Gibbs, H. L. (2021). Predicting migration routes for three species of migratory bats using species distribution models. *PeerJ*, 9.

Wieringa, J. G., Nagel, J., Campbell, C. J., Nelson, D. M., Carstens, B. C., and Gibbs, H. L. (2023). Combining stable isotopes, trace elements, and distribution models to assess the geographic origins of migratory bats. *Ecosphere*, 14(6):e4588.

Wieringa, J. G., Nagel, J., Nelson, D. M., Carstens, B. C., and Gibbs, H. L. (2020). Using trace elements to identify the geographic origin of migratory bats. *PeerJ*, 8:e10082.

Wilcove, D. S. and Wikelski, M. (2008). Going, going, gone: Is animal migration disappearing. *PLoS Biology*, 6(7):e188.

Wiser, R., Bolinger, M., Hoen, B., Millstein, D., Rand, J., Barbose, G., Darghouth, N., Gorman, W., Jeong, S., and Paulos, B. (2022). Land-Based Wind Market Report: 2022 Edition. Technical report, U.S. Department of Energy.

Wiser, R. and Bollinger, M. (2011). 2011 Wind Technologies Market Report. Technical report, U.S. Department of Energy.

Wood, S. N. (2011). Fast stable restricted maximum likelihood and marginal likelihood estimation of semiparametric generalized linear models. *Journal of the Royal Statistical Society: Series B (Statistical Methodology)*, 73(1):3–36.

Zazzo, A., Monahan, F. J., Moloney, A. P., Green, S., and Schmidt, O. (2011). Sulphur isotopes in animal hair track distance to sea. *Rapid Communications in Mass Spectrometry*, 25(17):2371–2378.

Zimmerling, J. R. and Francis, C. M. (2016). Bat mortality due to wind turbines in Canada. *The Journal of Wildlife Management*, 80(8):1360–1369.

Zuur, A. (2009). *Mixed Effects Models and Extensions in Ecology with R*. Statistics for Biology and Health. Springer New York, New York, NY, 1st ed. 2009. edition.